

ORNL/TM-11030

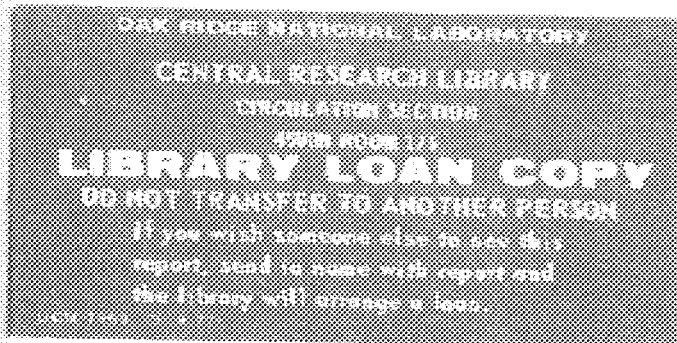
**OAK RIDGE
NATIONAL
LABORATORY**

MARTIN MARIETTA

**Feasibility Study and Developmental
Efforts for an Optical Detector
for Neutron Dosimetry**

Progress Report

S. R. Hunter
J. E. Turner
W. A. Gibson



OPERATED BY
MARTIN MARIETTA ENERGY SYSTEMS, INC.
FOR THE UNITED STATES
DEPARTMENT OF ENERGY

Printed in the United States of America. Available from
National Technical Information Service
U.S. Department of Commerce
5285 Port Royal Road, Springfield, Virginia 22161
NTIS price codes—Printed Copy: A04 Microfiche A01

This report was prepared as an account of work sponsored by an agency of the United States Government. Neither the United States Government nor any agency thereof, nor any of their employees, makes any warranty, express or implied, or assumes any legal liability or responsibility for the accuracy, completeness, or usefulness of any information, apparatus, product, or process disclosed, or represents that its use would not infringe privately owned rights. Reference herein to any specific commercial product, process, or service by trade name, trademark, manufacturer, or otherwise, does not necessarily constitute or imply its endorsement, recommendation, or favoring by the United States Government or any agency thereof. The views and opinions of authors expressed herein do not necessarily state or reflect those of the United States Government or any agency thereof.

MEMORANDUM OF PURCHASE ORDER B-T0290-A-X

Originating from
Battelle Pacific Northwest Laboratories
Post Office Box 999
Richland, Washington 99352

FEASIBILITY STUDY AND DEVELOPMENTAL EFFORTS FOR AN OPTICAL DETECTOR
FOR NEUTRON DOSIMETRY

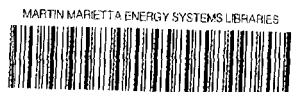
PROGRESS REPORT

By

S. R. Hunter,¹ J. E. Turner,¹ and W. A. Gibson²
¹Health and Safety Research Division
Oak Ridge National Laboratory
Oak Ridge, Tennessee 37831-6123
²Pellissippi International, Inc.
10521 Research Drive
Knoxville, Tennessee 37932

Date Published - January 1989

OAK RIDGE NATIONAL LABORATORY
Oak Ridge, Tennessee 37831
Operated by
MARTIN MARIETTA ENERGY SYSTEMS, INC.
for the
U.S. Department of Energy
Under Contract No. DE-AC05-84OR21400



Contents

Section		Page
I	Introduction.....	1
II	Background.....	1
III	Optical Electron Detection Technique.....	2
	3.1 Detector Concept.....	2
	3.2 Calculated Performance.....	5
IV	Milestone Accomplishments.....	7
	4.1 Observation of an Ionizing Particle Track in a Gas....	7
	a. Ionization Chamber.....	8
	b. RF High Voltage Generator.....	10
	4.2 Performance Evaluation of the Optical Detector.....	15
	a. Gas Mixture Studies.....	15
	b. Voltage Waveforms and Track Observations.....	17
	c. Photographic Recording of the Particle Tracks....	19
	d. Conclusion.....	20
V	Publications and Presentations.....	22
VI	Progress on Future Milestones.....	24
	6.1 Final Chamber Design.....	24
	6.2 Track Imaging Camera Characteristics.....	25
	6.3 Detector Operation and Analysis Software Requirements.	26
	6.4 High Voltage Pulsed RF Supply.....	27
	6.5 High Voltage Shock Exciter.....	27
	6.6 Particle Track Detection and Triggering Circuit.....	28
	6.7 Gas Mixture Optimization.....	30
VII	Conclusions.....	30
	References.....	32
	Appendices.....	33

Research sponsored by the Office of Health and Environmental Research and the Office of Nuclear Safety, U.S. Department of Energy, under contract DE-AC05-84OR21400 with Martin Marietta Energy Systems, Inc., and by the National Cancer Institute under Grant SSS-X(E) 1R43 CA45869-01 with Pellissippi International.

I Introduction

This report describes the progress that we have made during the period from the commencement of this study (June 28, 1988) up to October 31, 1988. During this period, we have successfully completed the first two milestones for this project. These were to fabricate and construct a simple ionization chamber, an associated vacuum system and to develop a pulsed RF high voltage source to excite the electrons in the particle track and to be used to test the optical detection technique. The observation and photographing of ionizing particle tracks in a gas was to constitute the successful completion of this milestone. The second milestone consisted of evaluating the performance of this simple detector as a guide to the design of a final version, in terms of the operating gas pressures and mixture composition used to optimize the light output, and the RF voltage pulse amplitude, frequency and duration to achieve optimal spatial resolution. This progress report which outlines our observations constitutes the successful completion of this milestone.

II Background

Fundamentally new concepts for the measurement of dose and LET of a variety of forms of ionizing radiation (and neutrons in particular) have recently been developed by us.¹⁻⁴ These concepts for neutron dosimetry are based on the digital, rather than analog, measurement of the charged-particle recoil tracks in an ionization chamber. Whereas present techniques utilize tissue-equivalent instruments and measurements of pulse height and shape to infer neutron dose and dose equivalent, the new methods register a charged-particle track by measuring the number of electrons it produces in given subvolumes of a chamber gas. The track is thus characterized by a set of

integers associated with each volume element. A digital detector of this type can measure both the track length and the energy deposition by observing the production of the secondary electrons in the path of a neutron recoil ion, enabling the identity of the recoil ion, as well as its energy and LET, to be established.

We have developed an ionizing particle track detector which can in principle determine the three-dimensional spatial distribution, with good resolution, of the secondary electrons produced in a gas by the passage of the ionizing radiation. This scheme is an optical method where the locations of the secondary electron tracks are imaged by the radiation produced in the excitation of the surrounding gas by the electrons in the particle track. This concept is outlined below along with the progress we have made toward the realization of this detector concept.

III Optical Electron Detection Technique

3.1 Detector Concept

The optical electron detection technique is based on an experimental device first developed by Cavalleri,⁵ and used by him to measure the concentration of electrons in low density discharge, from which he obtained estimates of thermal electron diffusion coefficients in several gases. A paper describing the present ionizing radiation detector concept has been published recently.¹ A schematic diagram of this device is given in Fig. 1 and may be described as follows:

Ionizing radiation (charged particle, recoil particle, laser beam, etc.) enters the detector through a window or converter material and collides with a low-pressure ($P \approx 0.1$ to 10 kPa) gas or gas mixture between two parallel metallic electrodes. The gas between the electrodes is ionized in collisions

with the high-energy primary radiation and secondary electrons to produce a track of low-energy electrons in the gas. A small continuous RF ($f \approx 10$ to 100 MHz) or DC field ($E/N \approx 0.1$ to 10.0×10^{-17} V cm²; E/N is the density-normalized electric field strength) is applied across the electrodes to "heat" the electrons in the track above thermal energy so as to prevent electron-positive ion recombination from removing electrons before imaging.

The high-energy ionizing radiation and secondary electrons will electronically excite as well as ionize the gas or gas mixture in the chamber, and the prompt decay of these excited atoms or molecules will produce a small burst of optical radiation which can then be detected by two wide angle, fast, high sensitivity photomultipliers. Signals from the photomultipliers are amplified and fed into a fast discriminator-coincidence detector where a trigger pulse is produced when two photomultiplier pulses are detected within a given coincidence window ($T \approx 0$ to 50 ns). This trigger pulse is fed into a master timing circuit which in turn triggers a high voltage (1 to 50 kV) highly damped (decay time $\tau \approx 100$ ns to 1 μ s) RF pulse generator ($f \approx 20$ to 100 MHz). The RF pulse from this generator is applied across the electrodes in the detector and excites the electrons in the particle track.

The RF field causes the electrons to rapidly oscillate, gaining sufficient energy to ionize and electronically excite the surrounding gas, and consequently, to produce a pulse of light whose intensity is directly proportional to the magnitude and duration of the RF pulse. The frequency of the pulse generator is adjusted such that the average energy of the electrons remains essentially constant during one period of the field (this sets the lower limit on the frequency), but at the same time the electron momentum follows the alternating field (i.e., low enough such that the electron experiences several collisions with the surrounding gas during one period of

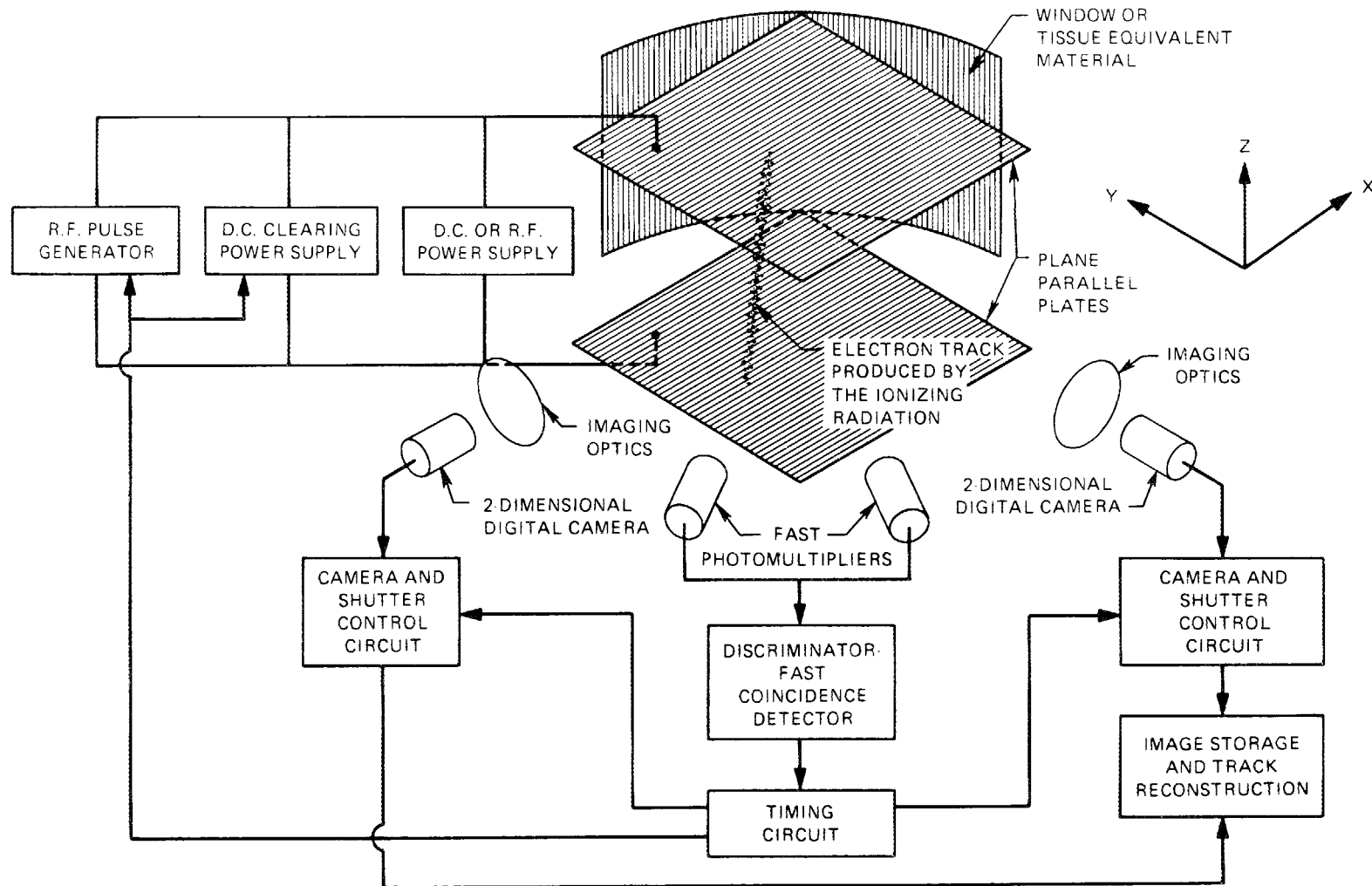


Fig. 1. Schematic diagram of the device using the optical detection technique which will be used in the final neutron dosimetry instrument.

the field). The gas within the detector is chosen to have a high gas-ionizing efficiency (i.e., low ionization threshold and W value) but more importantly to have a high quantum yield for the production of prompt (decay times $\lesssim 10$ ns) UV to visible (300 to 600 nm) radiation. The amplitude and duration of the RF pulse is chosen such that every electron in the track produces a detectable pulse of light in both of the detector cameras.

The two-dimensional digital detector cameras may either be silicon-intensified vidicon cameras or microchannel plate-intensified charge-coupled device (CCD) or similar semiconductor cameras. These cameras must have large pixel arrays ($\gtrsim 500 \times 500$ pixels) to accurately image the optical radiation produced by the excitation of the electrons in the detector. The resolution of the detector is proportional to the size of the pixel arrays in the camera. The cameras, which are triggered by a pulse from the master timing circuit have variable exposure times which are adjustable (10 ns to 1 μ s) to ensure that at least one detectable photon is recorded by both cameras for every electron in the track. The two cameras image the track in the x-z and y-z planes, and the digitally stored track image is transferred to a computer for permanent storage, track reconstruction, and analysis.

After the imaging of the particle track is complete, a small DC clearing field is applied across the detector electrodes to clear the electrons and ions from the detector chamber, and the detection circuits are reset to record a second particle track.

3.2 Calculated Performance

An analysis of the performance of this ionizing particle track detection technique has recently been made by Hunter.¹ The analysis indicates that each electron in the particle track is required to produce $\approx 10^5$ photons if the

detector is to image every electron in the particle track with high probability. This requirement governs the other operating parameters of the detector. Secondly, an analysis of the frequency requirements on the high voltage pulsed RF power supply indicated that if the field applied to the ionization chamber is within the frequency range $10 < f < 100$ MHz, then the transport and rate coefficients of the electrons within the track will be approximately time invariant. Under these circumstances it is possible to calculate the magnitude of the electron and photon growth in the particle track as a function of time, and also to estimate the decrease in spatial resolution (i.e. increase in the uncertainty that a photon observed by the digital cameras was produced at the position of production of the initial electron in the particle track) due to diffusion and drift of the electrons away from their initial positions of production.

Calculations of the rate of electron and photon growth were performed in N_2 which was chosen to illustrate the time development of these parameters as the relevant electron transport and rate coefficients are readily available. N_2 has a high production coefficient for near UV light (337-nm radiation from the second positive band [$C^3\pi-B^3\pi$]) which can be detected with intensified solid state cameras with good quantum efficiency. Pure nitrogen is not necessarily the optimum gas to choose in this application as has been observed in the studies which are summarized in this report in Section 4.2.

Calculations performed for typical discharge conditions (i.e. gas pressure = 10 kPa \approx 75 torr; $E/N = 200 \times 10^{-17}$ V cm² at high voltage field frequency = 30 MHz) indicated that approximately 10^6 photons would be produced in the discharge approximately 50 nsec after the application of the high voltage RF burst. Under these conditions the uncertainty in the position of production of the radiation in the discharge due to radial electron diffusion

due to the applied electric field was found to be ≈ 0.5 mm, and the drift of the electrons in the direction of the applied electric field was ≈ 1 to 2 mm. Operation at higher frequency electric fields was found to significantly reduce the displacement of the electrons away from the initial location of the particle track.

These calculations, although performed on an unoptimized gas mixture, did show that it is possible to image the electrons of an ionizing particle track with an uncertainty of ≈ 1 mm using the present optical electron detection technique. This uncertainty is sufficiently small, such that it is possible to use this concept to determine the identity and energy of the recoil particles produced in the interaction of high-energy neutrons with tissue-equivalent gases.

IV Milestone Accomplishments

4.1 Observation of an Ionizing Particle track in a Gas

A simple ionization chamber and associated vacuum system and gas handling manifold has been constructed and has been used to test the present optical detection method. A pulsed RF high voltage source has also been developed which we have used to excite the electrons in the particle track for visual observation. A schematic diagram of the present apparatus is given in Fig. 2, showing the method used for producing the ionizing particle tracks, and the resonantly tuned pulsed RF transformer circuit which was used to excite the electrons. Photographs of the actual apparatus and associated electronics are shown in Figs. 3 and 4. The development of the ionization chamber and the pulsed RF voltage source are described in detail below.

a. Ionization Chamber

The chamber was a 5 inch diameter Lucite cylinder with O-ring grooves turned in each end. A bottom plate of Al was used as one electrode and another Al or glass plate with a thin conductive coating of tin oxide was used as the top electrode (obtained from the Donnelley Corporation, Holland, Michigan). The tin oxide had a resistivity of about 50 ohms/sq cm and a light transmission in the visible of about 85% (including losses in the glass). The Lucite walls and glass electrode permitted nearly uninhibited viewing from all desired perspectives.

Three chambers were constructed with lengths of 1/2, 1, and 1-1/2 inches. The length of the chamber determined the distance between the electrodes and hence the field strength E for a given voltage between the plates ($E = V/d$, where V is the voltage and d is the distance between the electrodes). The field strength is a critical factor in the operation of the system, and it was found that the 1" chamber permitted operation near 500 mm of gas pressure with the voltage available. A gas pressure of 500 mm gave convenient alpha-particle track lengths of about 7 cm with sufficient vacuum to hold the electrodes firmly against the O-ring seals. Thus most investigations were carried out with the 1" chamber.

An Am^{241} source from a smoke detector was chosen since it was conveniently mounted on a small metal disk, had a near ideal strength of 1 microcurie, was safe, and was easily obtainable. The source was mounted in the side wall of the chamber to give good viewing of the tracks over a wide range of track lengths. This arrangement gave ≈ 3000 α -particles/sec into the chamber.

The vacuum system consisted of an oil diffusion pump backed by a mechanical roughing pump which allowed pressures of the order of 10^{-6} torr to be obtained. The chamber was usually flushed with Ar several times before

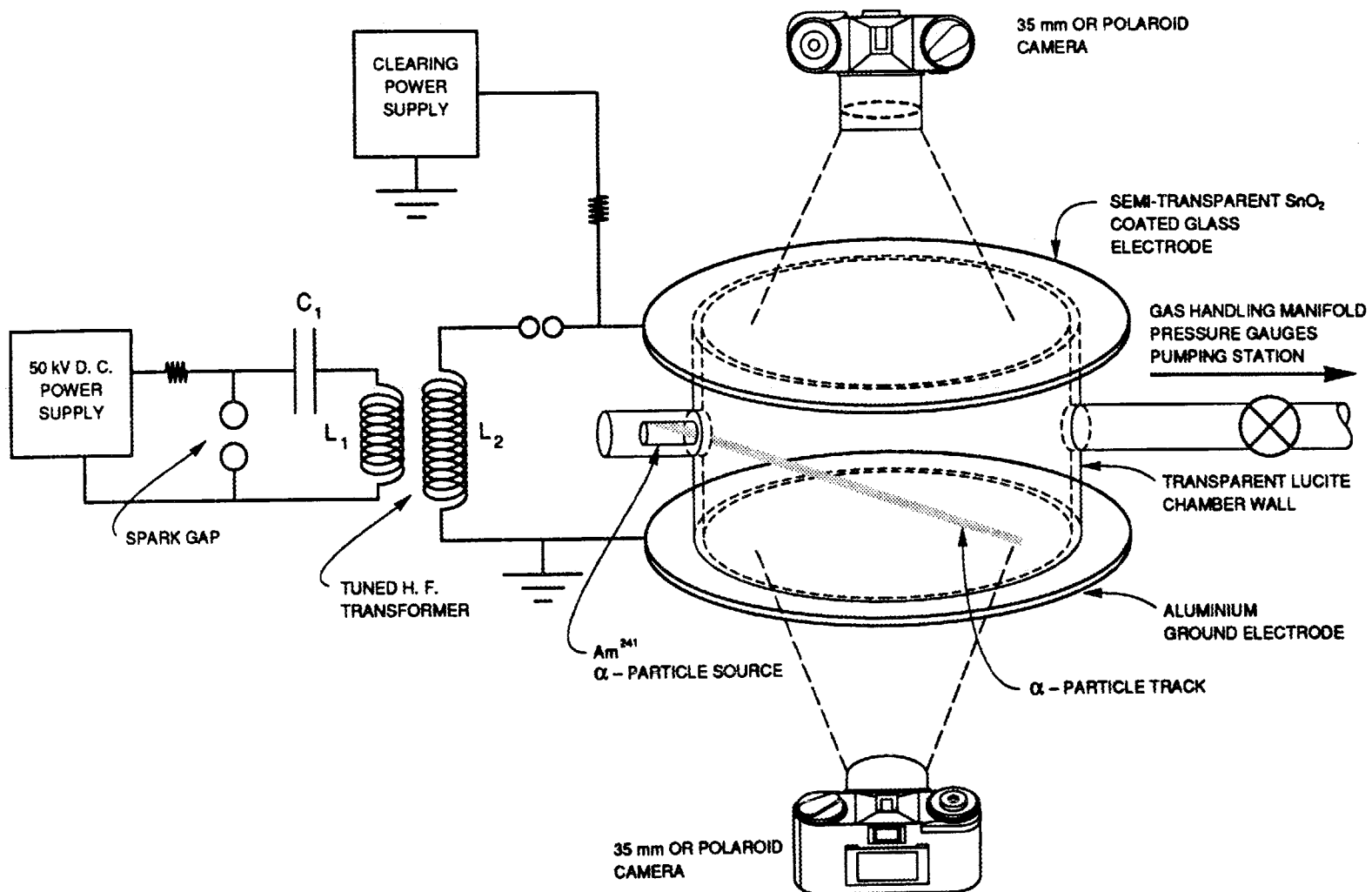


Fig. 2. Schematic diagram of the prototype device developed during this contract, showing the ionization chamber and the pulsed, resonantly tuned, high voltage, RF transformer circuit.

adding the final gas mixture in order to further reduce contaminants in the chamber. The presence of trace impurities, particularly pump oil and sealing grease, has been found to enhance the light output from the RF excited discharge in "pure" Ar. Consequently, it is necessary to clean the chamber as thoroughly as possible if the real effects of changes in gas mixture composition are to be observed.

b. RF High Voltage Generator

Various methods of generating the RF voltage were considered. It was desired to impress approximately 10-50 kV at a frequency of 10-20 MHz across the electrodes of the chamber. The capacitance of the chamber was calculated to be approximately 10 picofarads with an impedance of approximately 1500 ohms at 10 MHz. Thus the peak current would be over 10 amps, and the use of a continuously switched RF generator did not seem feasible because of the high power requirements. Since only a few cycles, at the most, were required, several pulsed voltage sources have been investigated for use as the high frequency, high-voltage source to excite the electrons in the particle track. These sources include a spark-coil-energized damped L-C oscillator, a shock-excited resonantly-tuned RF transformer circuit and a fast pulsed coaxial cable discharge circuit. Presently, we have been most successful with the resonantly-tuned transformer circuit, and have achieved pulsed high voltages (peak voltage \approx 10 kV) with resonant frequencies in the range 5-15 MHz, and pulse decay times of \approx 100 ns.

Once an alpha track is formed in the gas the electrons begin to diffuse rapidly and the RF field should be applied quickly ($<$ 100 nsec) to avoid track distortion due to electron diffusion. This can be done by detecting the track formation from the prompt photons weakly emitted by the atoms excited by the

alpha particle. However, since the objective was to demonstrate feasibility of track imaging, calculations showed that a randomly-triggered RF burst would result in adequately defined tracks for this purpose.

Based on the above criterion an automotive spark coil and spark module were selected for the high-voltage power supply and were triggered at approximately 100 Hz by a signal generator (Fig. 3 and 4). The voltage output of the coil was rated at 30 kV and had a risetime of about 100 μ s. The coil also proved to supply adequate energy for this application. The high voltage output of the coil charged the capacitor C_1 through the primary L_1 of a transformer (see Fig. 2). When the voltage on C_1 reached the breakdown potential of the spark gap conduction commenced in the gap in a few nanoseconds and the primary LC (i.e. L_1C_1) circuit resonated until dissipative losses damped out the oscillations. Oscillations in the primary of the transformer induce oscillations in the secondary resonance circuit which consists of L_2 and the capacitance C_c of the chamber. (Although they are significant, stray inductances and capacitances will be ignored in this analysis.)

In order to increase the energy transfer between the primary circuit and the secondary and to avoid distortion of the oscillations caused by beat frequencies, the primary and secondary circuit were independently tuned to the same resonance frequency. If this is done the circuit equations show that the tuned transformer system will resonate at two frequencies whose separation is determined by the mutual inductance between L_1 and L_2 . In shock excited circuits the lower frequency will dominate because the dissipative mechanisms are less than for the higher frequency mode. The tuning was accomplished by connecting a signal generator across L_1 and sweeping the frequency until the resonance was observed in the secondary. The observation was made by inductively coupling an oscilloscope loosely to the transformer with one loop

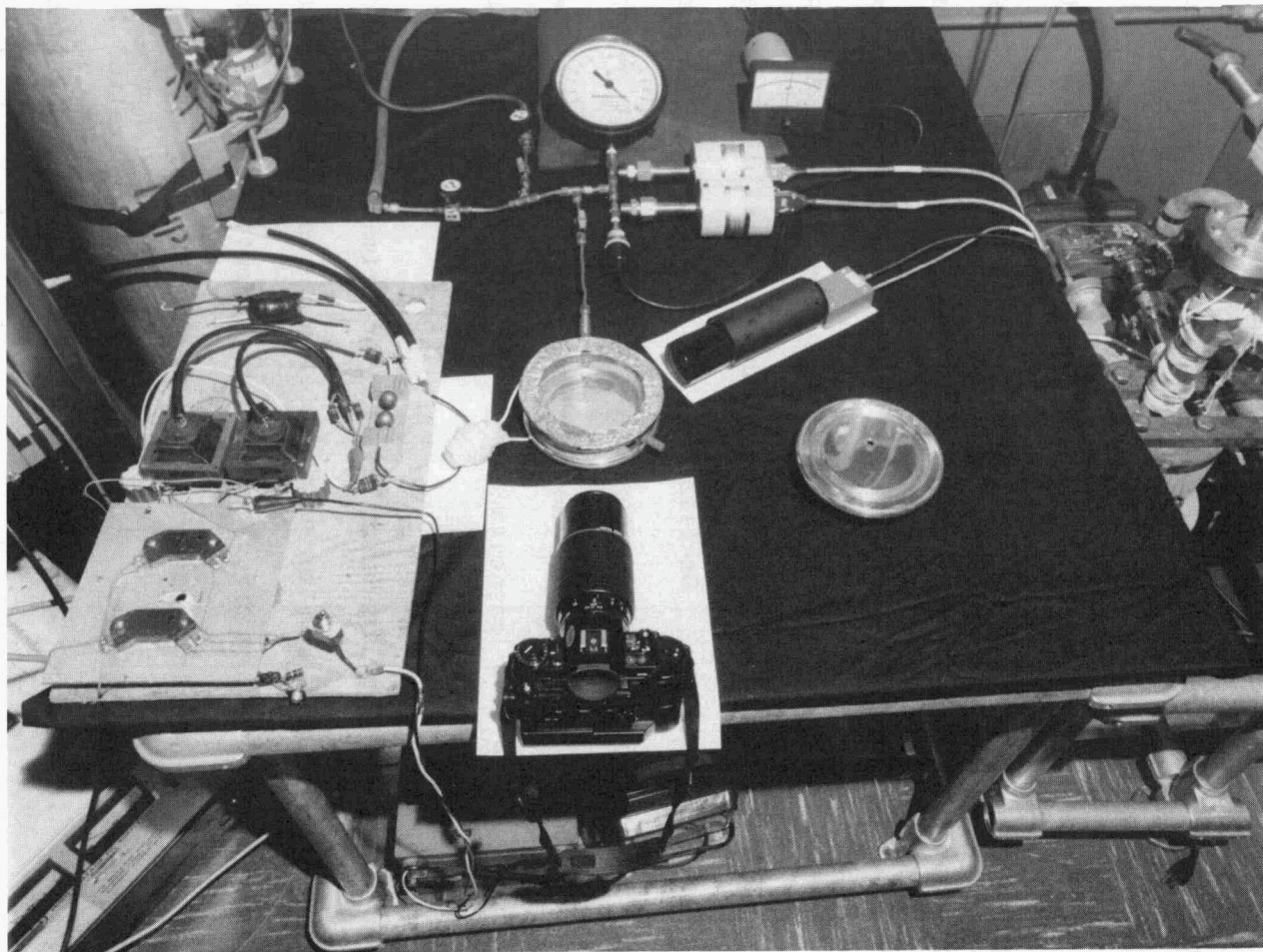


Fig. 3. Photograph of the prototype optical ionizing radiation detector, showing the spark-coil high-voltage circuit, ionization chamber, pressure gauges and gas-handling manifold, 35-mm camera and the photomultiplier and preamplifier for the high-voltage triggering circuit.



Fig. 4. Photograph of the optical ionizing radiation detector and the associated electronic and gas handling equipment.

of wire. The primary was then tuned by disconnecting the chamber and exciting L_2 with the signal generator and adjusting C_1 until the resonance of the primary circuit was just equal to that of the secondary. In order to complete the primary circuit the spark gap was shorted out during tuning. For convenience C_1 was a length of RG-8 coaxial cable which was reduced to the correct capacitance by trimming off the end (Fig. 3).

A number of transformers were wound on a 1" nonmagnetic core to investigate the effects of the inductance, turn ratios, and different diameter and materials of wire on the performance of the system. Two of these transformers are shown in Fig. 3. Tests were made with transformers with 4 primary and from 9 to 19 secondary turns. The transformers were made from various size wire of copper and nichrome. The use of nichrome wire introduces more resistance into the windings and broadens the tuning band (decreases the Q) and makes the transformer more tolerant to tuning errors at the expense of energy transfer to the chamber. The energy loss in the nichrome transformer appeared to be minimal, but the performance consistency seemed to be improved over all-copper transformers. It was concluded from the observations that the copper-wire transformer with 4 primary and 9 secondary turns and the nichrome-transformer with 4 primary and 19 secondary turns were the most satisfactory choices for this system. Track formation was observed with the various transformers for frequencies from 6 to 14 MHz; however, 11 MHz seemed near optimum for this setup. The coils of the transformer were independently tuned to approximately 13 MHz to obtain a lower system tune frequency of 11 MHz.

Figure 5 shows the calculated response of two inductively coupled LRC circuits which are shock excited and tuned to the same frequency and Fig. 6 shows the response of the coupled circuits when the individual circuits are

tuned to different frequencies. The calculations were performed using the solutions to the differential equations describing this system and are calculated in terms of relative amplitude vs. relative time. The distortion from a damped sine wave in the case of the untuned system (with resonant frequency ratios between the two circuits of 4:5) is caused by the beat frequency which is the difference between the resonant frequency of each of the circuits. The shape of the tuned and untuned calculated curves is similar to that observed on the oscilloscope with inductive pickup from a scope probe placed close to the chamber.

This ionization chamber and pulsed RF voltage source have been used in the study outlined below to observe the ionizing-particle tracks in various gas mixtures produced by the passage of an α -particle through the gas. The observation of the particle track in this chamber using the pulsed voltage source constitutes the successful completion of the first milestone.

4.2 Performance Evaluation of the Optical Detector

a. Gas Mixture Studies

Since the quantum efficiency and spectral response of light emission in the excited gas is dependent upon the gas and trace contaminants, several gases and gas mixtures were investigated. In most cases the majority of emitted energy is in the UV region which is not visible to the eye nor is the photographic film exposed to this radiation because of the absorption of UV in the walls of the chamber and camera lens (near total absorption of the UV took place at wavelengths below 360 nm with a small amount occurring in the visible blue). The following gases were tried: argon, nitrogen, xenon, propane, and TMAE (tetra-kis(dimethylamine)ethylene). Argon and nitrogen were utilized as the carrier gas with traces of the others added to enhance the light emission due to Penning ionization and excitation. Nitrogen was also added as a trace

Response of Coupled LRC Circuits

Tuned to Same Frequency

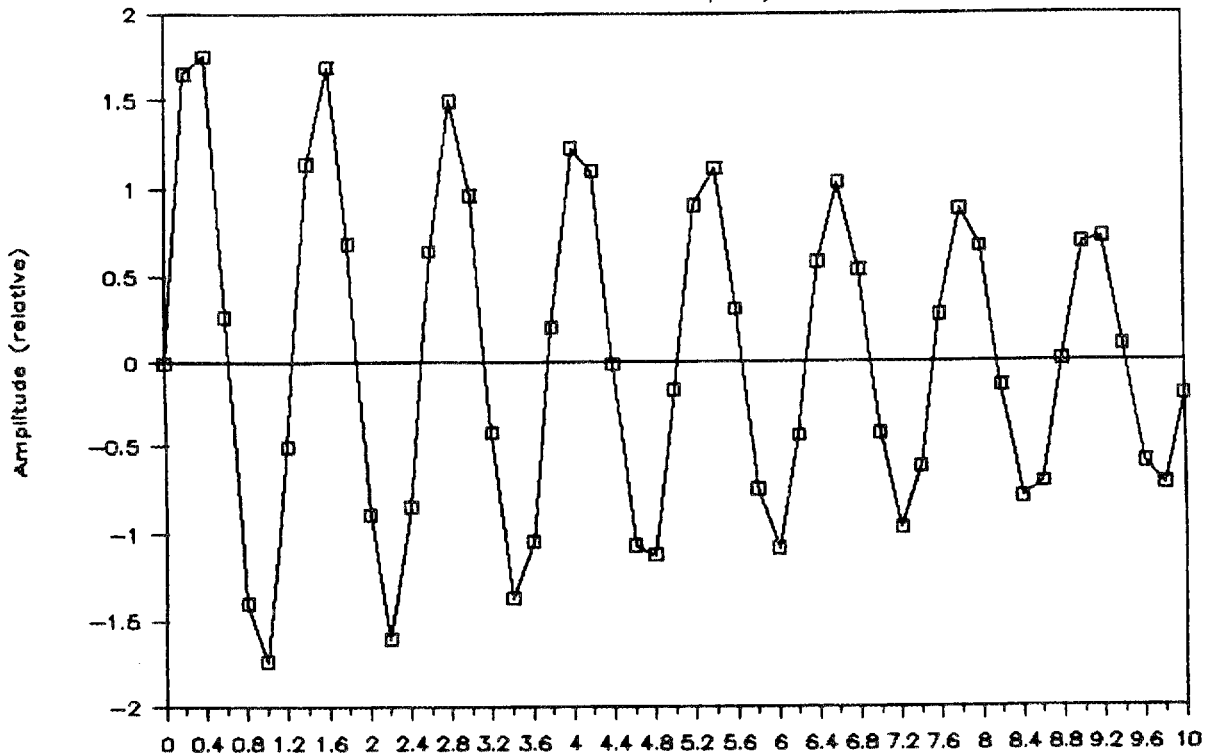


Fig. 5. The calculated response of two inductively coupled LRC circuits which are shock excited and tuned to the same frequency.

Response of Coupled LRC Circuits

Tuned Frequency Ratio 4/5

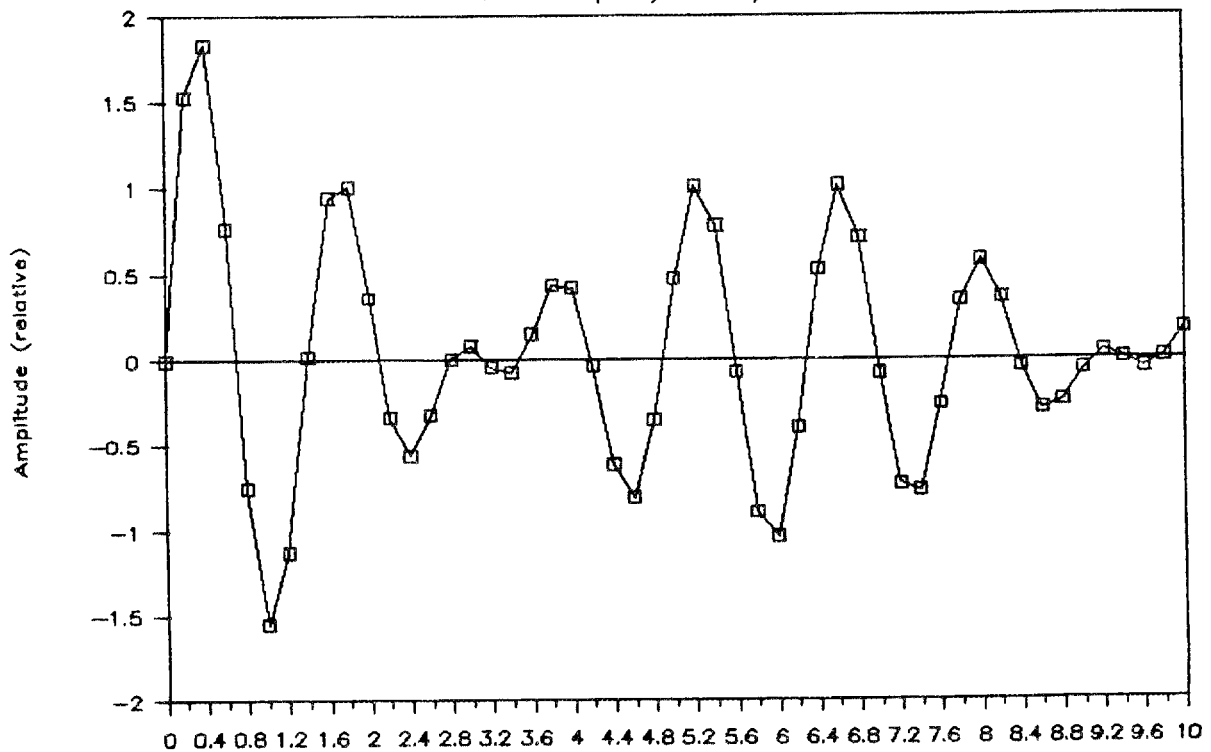


Fig. 6. The calculated response for the same circuits where the individual circuits are tuned to different frequencies.

gas to argon. It was found that for this investigation argon with approximately 1% xenon was a satisfactory mixture. TMAE is an interesting gas in that it has a very low ionization potential (5.4 eV vs. 15.7 eV for argon) and emits at 480 nm. This is near the peak of the spectral sensitivity of the eye and appeared to be the best trace gas from that standpoint. However, as described below the quantum efficiency was low in the near UV and was not a good choice for photographic recording. Inconsistent results were also initially obtained with "pure" Ar. At certain times we observed good light emission from the RF excited particle tracks. The light emission tended to decrease with better vacuum techniques and the flushing of the chamber with several fills of Ar. As a result, we attribute the optical emission to electronic excitation of trace quantities of vacuum pump oil and sealing grease in the "pure" Ar, which diminished in concentration when an improved vacuum system was used, or when the chamber was flushed with successive fills of Ar.

b. Voltage Waveforms and Track Observations

Due to the large amount of RF noise emitted by the spark gap, it was not possible to directly observe the voltage signal on the chamber with an oscilloscope. However, a good indication of the pulse shape, frequency and decay time of the signal impressed on the chamber could be obtained by simply placing the oscilloscope probe close to the chamber and observing the induced signal. The observed frequency was consistent with the lower tune frequency of the system as measured with a signal generator and the shape, if the tuning was accurate, was a damped sine wave. If the transformer was out of tune the signal was distorted with beats similar to that shown by the calculation graphed in Fig. 6. In any event the peak of the second oscillation was some

15% lower than the first, and further investigations indicated that the electronic excitation came primarily from the first cycle.

As the gas pressure was increased from approximately 30 microns to near atmospheric, the typical discharge regions were observed. At low pressure no discharge was observed, and as the pressure increased the onset of a glow discharge occurred. Then well-defined sparks were observed before the pressure reached the level that discharge no longer took place. With the alpha source in place, tracks defined by brilliant streamers consisting of well-defined discharges across the chamber were observed at the pressures where random sparks also occurred. As the gas pressure reached the levels where the random spark discharges and streamers extinguished, the well-defined alpha tracks could be easily seen as a diffuse blue glow. The gas pressure for optical track formation was critical, and pressure changes of a few percent were significant. Since the ratio of the electric field to the pressure P , E/P , is the parameter which characterizes the ionization rate in the gas, the observations indicate that the 15% reduction in this ratio during the second RF cycle resulted in an E/P too small for significant ionization and explains why track formation appeared independent of the decay time of the RF burst.

The tracks were as predicted by theory. Their length was defined by the range of the alpha track in argon and their diameter was approximately 2-6 mm as defined by electron diffusion prior to and during the approximately 90-nsec excitation period (1 cycle at 11 MHz). The track was shaped like a ball bat with the end larger than the beginning. It is thought that this is due to the greater ionization density produced as the alpha particles slow down.

c. Photographic Recording of the Particle Tracks

The tracks could be clearly seen by eye in a dark enclosure as a blue glow after one's eyes were well dark adapted. The tracks occurred at random times with an average period of seconds, depending upon the type of gas, voltage and gas pressure (and, of course, the source strength and solid angle of the particles entering the chamber). Since it was an objective to record the events photographically, the low light levels involved dictated that every effort be made to obtain the highest system sensitivity possible through the optimum selection of the film, lens, and processing techniques. Spectral emission data on argon and nitrogen⁶ predict that most of the light will be emitted in the UV over the wavelength region from 270 to 340 nm with only a very small amount in the visible region. However, the glass and plastic walls of the chamber and the glass in the lens will absorb most of the UV light at wavelengths less than 350 nm. Thus a high-speed film should be chosen with good sensitivity in the blue and UV at 350 nm and above to record what light there is. Furthermore, the film should be push developed with a high-contrast developer with pre-exposure.

Several film types were tried: Kodak Kodacolor VR-1000, Kodak T-Max P3200, Kodak 2475 recording, Konica 3200 color negative, and Polaroid 610 print. Of all of the film tested, Kodak 2475 proved to be the best even though it did not have the fastest ASA speed (e.g., ASA 1000 vs. ASA 20,000 for Polaroid 610). Film speeds are indicative of the sensitivity for defined applications and processing.⁷ In this case the superior blue and UV response of Kodak 2475 and the ability to push develop the film made it much more sensitive for this application than the Polaroid 610 and the two color films. In the case of the T-Max P3200 spectral sensitivity data is not available below 400 nm;⁸ however, it appeared to be inferior to that of Kodak 2475. In

no case did pre-exposure appear to provide a noticeable increase in speed, and the explanation for this observation is not known. (Pre-exposure to a uniformly illuminated surface increases the background density of the film so that any additional exposure occurs on a linear and higher-speed portion of the characteristic density vs. log [exposure] curve.)⁹

Exposures were made with a 35 mm camera with a f1.4 lens (except for the Polaroid exposures made with a Tektronix scope camera with an f1.8 lens) by opening the shutter and then closing it after visual observation of a track. In most frames no tracks were seen on the negative due to the low light level; however, a few showed discernible tracks. Prints of these tracks were nearly invisible and would not be effective in illustrating the results for this report. Through cooperation with the Engineering Department of the University of Tennessee, the negatives were digitized and the image was enhanced with image-enhancement software developed by Perceptics, Inc. A typical enhanced track is shown in Fig. 7. The top left hand corner image shows the unenhanced digitized image obtained from the 35-mm film. The top right-hand corner image is an enhanced image with a grey scale of 256, while the two lower images show the enhancement with a grey scale of 2; i.e. black and white.

d. Conclusions

This investigation demonstrated that a charged-particle track can be optically imaged utilizing the technique described. Visual observation of tracks were made over gas pressure ranges of 250 mm to 600 mm, and it was concluded that visible tracks could be formed at both lower and higher pressures with the appropriate equipment and E/P ratios. As the work progressed it became apparent that the electron excitation resulted mainly



Fig. 7. Photograph of a digitally-enhanced ionizing-particle track in a gas mixture of 1% Xe in Ar. The particle track was produced by the passage of a 5.5-MeV α -particle through the gas mixture at a total gas pressure of ≈ 500 torr. The particle track starts at the top right hand corner of each image and ends near the center of the chamber. The total track length was ≈ 5 cm and the width of the track was ≈ 3 -4 mm.

from the first RF cycle or possibly from the first half of that cycle. The signal appeared to decay sufficiently during subsequent cycles that they played a minor role in the excitation. It was finally concluded that tuning was not as important as originally thought and, as shown in Figs. 5 and 6, detuning has little effect on the first cycle. In order to increase the light output during subsequent cycles it appears necessary to have an RF burst having equal amplitude oscillations rather than an exponentially decaying burst which occurred in the present developmental effort. Of course excitation during successive cycles increases the diffusion time and thus degrades the track definition. Our subsequent studies will examine these conflicting requirements in detail.

It is anticipated that with UV-sensitive or intensifying-imaging devices even the low-light-level track could be easily recorded and by triggering the RF excitation on the event, to reduce electron diffusion and absorption effects, better defined and brighter tracks would be observed. Higher RF frequencies should also improve the track resolution.

V Publications and Presentations

The following presentations and papers have been published acknowledging the sponsorship of both OHER and the Office of Nuclear Safety.

1. Modeling studies and progress on the development of a prototype detector used for the design of the present detector were reported in two papers which were presented at the annual Health Physics Society meeting in Boston on July 4 to July 8. These papers acknowledged partial support from the Office of Nuclear Safety. The titles and authors were:
 - a. "The Development of an Optical Ionizing Radiation Track Detector,"
S. R. Hunter, W. A. Gibson, G. S. Hurst, and J. E. Turner.

- b. "Applications of an Optical Ionization Radiation Track Detector in Neutron Dosimetry and Microdosimetry," H. A. Wright, J. E. Turner, W. E. Bolch, R. N. Hamm, G. S. Hurst, and S. R. Hunter.
2. An invited presentation entitled "Development of an Optical Ionization Chamber" by J. E. Turner, S. R. Hunter, R. N. Hamm, H. A. Wright, G. S. Hurst, and W. A. Gibson was given at the Workshop on the Implementation of Dose Equivalent Meters Based on Microdosimetric Techniques in Radiation Protection, Schloss Elmau, FRG, October 18-20, 1988. A paper based on this presentation has been written and will be published as an invited paper in the proceedings of the workshop in the journal *Radiation Protection Dosimetry*. A copy of this paper is given in Appendix A.
3. A contributed paper entitled "Design Criteria for an Optical Ionizing Radiation Particle Track Detector" by S. R. Hunter, W. A. Gibson, and G. S. Hurst was presented at the 41st Gaseous Electronics Conference, Minneapolis, Minnesota, October 18-21, 1988. The abstract of this paper will be published in the Bulletin of the American Physical Society in 1989.
4. An invited paper entitled "Digital Characterization of Recoil Charged-Particle Tracks for Neutron Measurements" by J. E. Turner, S. R. Hunter, R. N. Hamm, H. A. Wright, G. S. Hurst, and W. A. Gibson has been written. This paper was presented at the 10th Conference on the Application of Accelerators in Research and Industry, Denton, Texas, November 7-9, 1988, and has been accepted for publication as a refereed article in the journal *Nuclear Instruments and Methods*. A copy of this paper is given in Appendix B.

5. An abstract entitled "Analysis of Data from an Optical Ionizing-Radiation Track Detector" by R. N. Hamm, J. E. Turner, H. A. Wright, S. R. Hunter, G. S. Hurst, and W. A. Gibson has been submitted for consideration as a contributed paper at the 37th Annual Meeting of the Radiation Research Society, Seattle, Washington, March 18-23, 1989.
6. Two abstracts have been submitted for consideration as contributed presentations at the 10th Symposium on Microdosimetry to be held in Rome, Italy, May 21-26, 1989. These abstracts are entitled a) "An Optical Electron Detection Technique for the Observation of Ionizing Radiation Particle Tracks in a Gas" by S. R. Hunter, W. A. Gibson, G. S. Hurst, H. A. Wright, J. E. Turner, and R. N. Hamm, and b) "Analysis of Data from an Optical Ionizing-Radiation-Track Detector" by R. N. Hamm, J. E. Turner, H. A. Wright, S. R. Hunter, G. S. Hurst, and W. A. Gibson.

VI Progress on Future Milestones

6.1 Final Chamber Design

We are presently discussing the relative merits in the development of either a neutron spectrometer or a neutron dosimetry device as the next logical step in this detector development study. The material requirements on the walls and the chamber gas for a spectrometer are less severe than those required in neutron dosimeters, and consequently, the chamber walls and electrodes can be constructed of quartz. The principal advantages of using quartz are that it is transparent to the UV radiation produced in the RF excitation of the electrons in the particle tracks and also the incident neutrons will have a small cross section for interacting with the walls of the detector. Similarly, since tissue-equivalent counting gases are no longer required, a more appropriate chamber gas appears to be He, with the addition

of small quantities (\lesssim 5%) of heavier rare gases (i.e. Ar, Kr or Xe) or molecular additives (e.g. N₂, TEA, TMAE) to increase the rate of ionization (by Penning ionization, for example) and UV to visible radiation from the RF-excited particle tracks in the gas. Discussions regarding the final chamber design are continuing and will be outlined in later reports.

6.2 Track Imaging Camera Characteristics

Potentially, the most expensive items required for the neutron detector are the imaging cameras. The expense of these cameras is very much a function of the sensitivity required in a given application (which is directly related to the amount of light produced in the excitation of the electrons in the particle track). Presently commercially available CCD cameras having the required resolution (i.e about 500 × 500 pixel array) with a detection threshold of about 3 lux and used in consumer products, cost about \$1,000. Image-intensified night-surveillance cameras, with a threshold sensitivity of 10⁻³ lux are commercially available for about \$10,000 while high-gain image-intensified cameras for scientific and defense applications with a threshold of about 10⁻⁶ lux (corresponding to single photon sensitivities) are available from limited sources for about \$20,000 for one camera exclusive of the data-acquisition system and software. It is obvious then, that if sufficient light can be generated in the discharge, a lower-cost camera (and hence a more commercially acceptable product) can be used in the particle-track detector.

The spectral and quantum efficiency characteristics required of the cameras has to be closely matched with the frequency of the radiation produced in the discharge for optimal detector performance. The use of high-speed electronic shutters (shutter speeds up to 50 nsec) is being examined as a means for reducing background noise and stray light in the camera (i.e.

increasing the signal to noise ratio in the camera's video output). High-speed gating of the cameras' shutters will also be used to improve the resolution of particle-track image by rejecting unwanted "late" radiation produced in the discharge at times longer than required to produce enough radiation to image the positions of the electrons in the particle track. The array size used in the cameras is determined primarily by the resolution with which the electrons in the particle track are to be imaged. The data-collection rate, memory and computing speed requirements of the image-analysis computer and consequent system cost are also functions of the array size. Commercially available camera systems commonly have pixel array sizes of about 500×500 although cameras with array sizes much smaller, and up to 2000×2000 pixels are available. A careful analysis is being performed to determine the optimal requirements on the cameras for the specific applications in neutron spectrometry and dosimetry in which the present technique can be used to advantage. This analysis will also be discussed in detail in later reports.

6.3 Detector Operation and Analysis Software Requirements

Several software packages will be required to operate the detector. Specifically, these include timing and synchronization signals, camera operation controls, video-image transfer and storage and three-dimensional image reconstruction of the particle track in the gas for final data analysis. Several of these packages can be purchased from commercial vendors, but considerable software development is still required, particularly in the reconstruction and analysis of the particle track. The image-analysis routines are presently being developed by J. E. Turner, R. N Hamm, and

H. A. Wright in the Health and Safety Research Division at the Laboratory. This work is being funded by the Office of Health and Environmental Research, Department of Energy.

6.4 High-Voltage Pulsed-RF Supply

The spatial resolution of the detector is directly related to the frequency of the applied high-voltage RF field. Presently, the device we have developed operates over a frequency range $f \approx 5$ to 15 MHz. We plan to study techniques for increasing the operating frequency to $f \approx 20$ to 30 MHz, which will significantly reduce the maximum excursion of the electrons in the particle track during each half cycle of the applied electric field. We plan to study carefully designed shock-excited L-C resonant circuits, tuned resonant transformer circuits, and coaxial-cable delay lines. Particle-track resolution and discharge light output can be maximized by optimizing the frequency, voltage level, and duration of the RF burst from these circuits. The optimization procedures for these circuits will form a significant part of the effort during FY 89 and FY 90.

6.5 High-Voltage Shock Exciter

Currently, a randomly triggered spark gap is used to shock excite the resonant circuit (see Fig. 2). Although this excitation scheme has the inherent advantages of simplicity and low cost, the present design cannot be triggered externally, and consequently, cannot be used in a practical neutron spectrometer where it is crucial that the high voltage RF burst be triggered immediately after the presence of a particle track is detected in the discharge chamber. A fast, high-voltage pulse source is being considered which can be used to trigger the high-voltage spark gap.

Alternatively, we are also studying the possibility of using a triggered high-current thyatron as the high-voltage exciter. The advantages of a thyatron are that fast trigger pulses (risetimes < 10 nsec) are easier to generate than for spark gaps (trigger voltages are about 500 V for a thyatron and < 5 kV for a spark gap), thyatrons can be turned on for a finite time (> 50 nsec) allowing accurate control of the RF high-voltage burst duration to be obtained, and finally, thyatrons produce considerably less RF electromagnetic (e.m.) noise than spark gaps. It is important to minimize the production of e.m. interference in the instrument as it will interfere with the operation of other circuits in the detector.

6.6 Particle-Track Detection and Triggering Circuit

A major area of developmental effort is required to devise efficient methods for detecting the presence of the ionizing particle as it enters the discharge chamber. It is vital for high-resolution imaging of the particle track that the high-voltage RF burst be applied across the chamber as quickly as possible after the ionizing particle track has been produced in the discharge chamber. We plan to detect the prompt fluorescence produced by the decay of molecules or atomic gases within the discharge chamber, excited by the passage of the ionizing particle through the gas. Due to the approximate equality of the total ionization and excitation cross sections in many gases at electron energies above about 50 eV, we expect approximately equal numbers of excitation and ionization events to occur within the discharge chamber (i.e. approximately 3.8×10^4 ionizing events in argon for a 1-MeV ionizing particle which completely stops in the discharge chamber). Calculations also show for typical photomultiplier and discharge chamber geometries, that the production of about 200 photons in the particle track will be sufficient to

produce at least one detectable photon at a wide viewing angle photomultiplier (Figs. 1 and 3). The coincidence, discriminator and timing circuits shown in Fig. 1 will be based upon commercially available units.

Presently, we have purchased a high-gain, fast photomultiplier with good sensitivity to optical radiation over the wavelength range $160 \text{ nm} \leq \lambda \leq 600 \text{ nm}$. The associated equipment for a photon counting system, including a preamplifier, discriminator/amplifier and power supply, have also been purchased (Figs. 3 and 4) and will be used to observe the fluorescence produced in the gas by the passage of the ionizing particle. It will be used in determining the detection efficiency by counting the number of observed particle tracks in conjunction with an electrical pulse-counting circuit. Optical emission intensities from the RF excited gas will also be quantified for different gas mixtures and excitation parameters. This equipment will eventually be used to produce a trigger pulse for the pulsed high-voltage RF supply and the imaging cameras. These studies are continuing.

For low-energy ionizing radiation, or low-LET radiation (e.g. X rays), there may not be enough prompt fluorescence produced in the gas to be used as a reliable trigger source and under these circumstances, an alternate event trigger is required. One possible trigger detector is a scintillator placed immediately in front of or at the back of the discharge chamber. The ionizing radiation, upon entering or leaving the discharge chamber, will lose part of its initial energy traversing the scintillator, producing a burst of light which can then be detected by a photomultiplier and used as a timing pulse. Studies of these concepts are also being made.

6.7 Gas Mixture Optimization

An area where potentially considerable improvements can be made in the sensitivity and, to a lesser extent, resolution of the detector is in the careful choice and tailoring of the gas mixtures used in the discharge chamber. We have already shown that certain gas mixtures work considerably better than others in terms of producing visible radiation when subjected to a high-voltage RF burst. Specifically, pure Ar produced little visible radiation, and operation was achieved only at comparatively low gas pressures for a given applied voltage and discharge chamber length. In contrast, the addition of about 1-5% Xe to the gas mixture allowed operation at considerably higher gas pressures, accompanied by enhanced production of visible radiation. The particle tracks were readily observable with this gas mixture. Our present observational and photographic capabilities are limited to the near UV and visible region of the spectrum ($\lambda > 360$ nm), whereas the predominant source of radiation produced in excitation of N_2 and a number of other candidate gases is predominantly in the UV region of the spectrum ($\lambda = 200-400$ nm). Considerable improvements in sensitivity can be expected when UV sensitive radiation detectors are used to image the light produced by selected gas mixtures and by constructing the chamber of UV-transmitting materials. A large part of the effort in FY 89 and FY 90 will be devoted to searching for gas mixtures and mechanisms (e.g. Penning ionization and excitation processes) which will maximize the production of radiation of wavelengths where the detector cameras have the highest quantum efficiency.

VII Conclusions

In this report we have summarized the progress we have made on the development of the optical electron detection technique for use in neutron

spectroscopy and dosimetry. In particular, we have successfully completed the first two milestones of this contract; namely the construction and successful operation of a prototype device with which we have been able to photograph the ionization track produced by the passage of a 5.5 MeV α -particle through a gas. Secondly, optimization studies have been performed in which we have attempted to maximize the light output from the RF-excited particle track while minimizing the loss in spatial resolution of the observed track, in the directions both perpendicular and parallel to the applied electric field. In these studies, three different techniques for generating the pulsed high voltage RF electric field have been examined. The resonantly-tuned shock-excited L-C transformer circuit shown in Fig. 2 was found to produce the best voltage waveforms, and values for the operating frequency and voltage amplification were found which produced the optimally spatially-resolved images of the ionization track in the chamber gas mixture. Studies were also performed with different gas mixtures operating over a range of gas constituent concentrations, total gas pressures and voltage pulse amplitudes, in attempts to optimize the production of visible light from the RF-excited particle tracks.

Several presentations and publications have directly resulted from this work, and are listed in Section V. Further publications and presentations are anticipated as a result of progress that has been made using this concept.

Finally, substantial progress has been made on the future milestones incorporated in this project. These include refining and characterizing the final radiation detector concept, including the associated pulsed-voltage and imaging-camera equipment. The most promising paths for enhancing the performance of the detector have been identified and will be pursued during

the next stage in the development of the optical electron detection concept for applications in the fields of neutron spectroscopy and dosimetry.

References

1. S. R. Hunter, "Evaluation of a Digital Optical Ionizing-Radiation Particle-Track Detector," *Nucl. Instr. Methods A260*, 469 (1987).
2. J. E. Turner, R. N. Hamm, G. S. Hurst, H. A. Wright, and M. M. Chiles, "Studies of a Digital Approach to Neutron Dosimetry and Microdosimetry," *Proc. 5th Symp. on Neutron Dosimetry*, EUR 9762 (CEC, Luxembourg), p. 675 (1984).
3. J. E. Turner, R. N. Hamm, G. S. Hurst, H. A. Wright, and M. M. Chiles, "Digital Characterization of Particle Tracks for Microdosimetry," *Radiat. Prot. Dosim.* **13**, 45 (1985).
4. Wesley E. Bolch, J. E. Turner, R. N. Hamm, H. A. Wright, and G. S. Hurst, "A Method of Obtaining Neutron Dose and Dose Equivalent from Digital Measurements and Analysis of Recoil-Particle Tracks," *Health Physics*.
5. G. Cavalleri, *Phys. Rev.* **179**, 186 (1969).
6. G. Charpak, W. Dominik, J. P. Fabre, J. Gaudaen, F. Sauli, and M. Suzuki, *Nucl. Instr. and Methods in Phys. Research A*, **269**, 142-148 (1988);
G. Charpak, W. Dominik, J. P. Farbre, J. Gaudaen, V. Peskov, F. Sauli, A. Breskin, R. Chechik, and D. Sauvage, *Some Applications of the Imaging Proportional Chamber*, *IEEE Transactions on Nucl. Sci.* **35**, No. 1, Feb. (1988).
7. "High-Speed Photography," Pub. No. G-44, Eastman Kodak Co., Rochester, New York.
8. "Kodak T-Max Professional Films," Pub. No. F-32, Eastman Kodak Co., Rochester, New York.
9. A. Adams, "The Negative," Little, Brown and Co., Boston (1983).

APPENDIX A

"DEVELOPMENT OF AN OPTICAL DIGITAL IONIZATION CHAMBER"

J. E. Turner, S. R. Hunter, R. N. Hamm, H. A. Wright
Oak Ridge National Laboratory
Post Office Box 2008
Oak Ridge Tennessee 37831-6123

G. S. Hurst and W. A. Gibson
Pellissippi International
10521 Research Drive
Knoxville, Tennessee 37932

To be published in the journal of *Radiation Protection Dosimetry*

DEVELOPMENT OF AN OPTICAL DIGITAL IONIZATION CHAMBER¹

J. E. Turner, S. R. Hunter, R. N. Hamm, H. A. Wright, Oak Ridge National Laboratory, Post Office Box 2008, Oak Ridge, TN 37831-6123 USA; G. S. Hurst and W. A. Gibson, Pellissippi International, 10521 Research Drive, Knoxville, TN 37932 USA.

We are developing a new device for optically detecting and imaging the track of a charged particle in a gas. The electrons in the particle track are made to oscillate rapidly by the application of an external, short-duration, high-voltage, RF electric field. The excited electrons produce additional ionization and electronic excitation of the gas molecules in their immediate vicinity, leading to copious light emission (fluorescence) from the selected gas, allowing the location of the electrons along the track to be determined. Two digital cameras simultaneously scan the emitted light across two perpendicular planes outside the chamber containing the gas. The information thus obtained for a given track can be used to infer relevant quantities for microdosimetry and dosimetry, e.g., energy deposited, LET, and track structure in the gas. The design of such a device now being constructed and methods of obtaining the dosimetric data from the digital output will be described.

¹Research sponsored by the Office of Health and Environmental Research and the Office of Nuclear Safety, U.S. Department of Energy, under contract DE-AC05-84OR21400 with Martin Marietta Energy Systems, Inc. and by NCI under contract with Pellissippi International.

Introduction

The title of this workshop brings together two aspects of radiation research: the science of microdosimetry and the practice of personnel radiation protection through the use of dose equivalent. The two are historically related through the measurement of LET distributions by microdosimetric methods as pioneered by Rossi⁽¹⁾. Today, microdosimetry is playing a fundamental role in the consideration of the most suitable reference variable for quality factors and the general expression of radiation quality for radiological protection. Microdosimetry also encompasses the study of fluctuations in energy deposition on a scale of cellular and subcellular - even molecular - dimensions. It is basic to our understanding of instrument response and of cavity and interface problems.

Calculations of charged-particle track structure have become an important part of microdosimetry. It is through such calculations that many measurements are analyzed, evaluated, and compared. Radiations of different quality, for instance, can be characterized in terms of their calculated proximity functions, giving the distribution of distances between ionizations in the track of a particle in a gas or in tissue. By way of example, Fig. 1(a) shows a track segment of a 5-MeV alpha particle in liquid water, calculated with the Monte Carlo computer code OREC⁽²⁾. Each dot shows the position of a subexcitation electron, one with an energy less than the assumed threshold of 7.4 eV for electronic transitions in liquid water. This spatial pattern of secondary electrons is formed rapidly (in $\sim 10^{-15}$ s) in the wake of the traversing alpha particle. For contrast, Fig. 1(b) shows the tracks of 1-keV electrons. The figure represents two examples of energy deposition

patterns by radiation. Microdosimetry addresses the ultimate differences in the physical, chemical, and biological effects of radiation in terms of track structure.

While such calculations are a cornerstone of microdosimetry, they are subject to uncertainties that have not been evaluated experimentally. For example, measurements of inelastic and elastic scattering cross sections for low-energy electrons in gases and, especially, in water or tissue are almost wholly lacking. Nevertheless, calculations based on various models can be very useful.

This paper describes the development of a new type of radiation detector which could, in principle, determine the three-dimensional spatial distribution of electrons in the track of a charged particle in a gas. The device is based on the detection of secondary electrons by optical means. Specifically, we hope to measure the numbers of electrons in various volume elements of a gas immediately after traversal by a charged particle. The electron numbers would provide a digital description of the track. Such an instrument would provide measurements for direct comparison with track-structure calculations. Moreover, as discussed below, the principle would have potential uses for measurements of a variety of important quantities for physics and dosimetry. At the present time we have constructed a device in which we have visually observed and photographed alpha-particle tracks. The device and its operation and our plans for continuing development of a digital chamber are described.

Optical Detection of Charged-Particle Tracks

The simple, preliminary device that we have used to optically observe ionizing tracks is shown schematically in Fig. 2. A ^{241}Am source ($\sim 1 \mu\text{Ci}$,

from a smoke detector) emits a 5.5-MeV alpha particle into the chamber gas, leaving a trail of subexcitation electrons in its path. An external, high-frequency (~ 10 MHz), high-voltage (~ 20 kV) pulse is applied at intervals of ~ 0.01 s across two disc-shaped electrodes on either side of the track. The application of the RF field is not triggered by the passage of the alpha particle in the present chamber, but will be in a later device. However, if the RF field happens to be applied immediately after the passage of the alpha particle, then the field rapidly accelerates the electrons back and forth in the particle track, causing them to ionize and excite gas molecules in their immediate vicinity. The excited gas molecules emit light in the UV to visible range by fast fluorescent decay in sufficient quantities for detection. Under suitable conditions, the amount of light from different portions of the track is proportional to the number of subexcitation electrons there, thus providing the basis for a digital characterization of the track. Tracks are readily visible to the naked, dark-adapted eye.

Figure 3 shows a photograph of an alpha-particle track from the ^{241}Am source. The particle starts from the upper right in each panel and stops in the lower left-hand region, where the track is the most dense. The track is about 5 cm long and 3-4 mm in width. The "raw" photograph is shown in the upper left-hand panel. As described in the next section, the panel in the upper right shows the track after it is digitally enhanced. The bottom two panels in the figure, which are identical, are obtained from the picture in the upper right with further enhancement.

Operation of First Chamber

The chamber in Fig. 2 is cylindrical in shape with a height of 3 cm and a diameter of 10 cm. A bottom plate of aluminum is used as one electrode and an

upper plate of tin-oxide coated glass is used as the other. The walls are made of transparent Lucite, permitting viewing of the tracks from the sides as well as from above. The ratio of the field strength and pressure (E/P) is a critical factor in the operation of the system. For a given voltage across the electrodes, this can be changed by changing their separation or the gas pressure in the chamber. Various combinations of gases and pressures were tried. A gas pressure in the neighborhood of 500 torr conveniently gives alpha-particle track lengths of about 7 cm and sufficient vacuum to secure the electrodes firmly to their O-ring seals. The chamber was usually operated at pressures between 300 and 600 torr. It was found necessary to evacuate the chamber to less than 10 mtorr before filling in order to remove contaminating gases, particularly oxygen.

The quantum efficiency and spectral response of light emission from the excited gas depends on the gas and its trace contaminants. Several combinations of gases and pressures have been tried: Ar, N_2 , Xe, propane, and TMAE (tetrakis(dimethylamine)ethylene). Argon and nitrogen were used as carrier gases with traces of the other gases added to increase Penning ionization and excitation processes. Nitrogen was also tried as a trace gas in argon. In most cases, the major portion of the light from the excited gas is emitted as UV, which is absorbed in the walls of the chamber and is not visible to the eye. TMAE has a very low ionization potential (5.4 eV vs. 15.7 eV for Ar) and emits visible light of wavelength 480 nm. However, its quantum efficiency is low. It was found that argon with ~1% xenon was the optimum gas mixture in the present experimental apparatus.

The RF field requirement is approximately 20 kV at a frequency of 10 MHz across the chamber electrodes in Fig. 2. The capacitance of the chamber is around 10 pF, and consequently the impedance is $\approx 1500 \Omega$ at 10 MHz. Thus a

peak current in excess of 10 A is needed, but only for a few cycles. For the first device we decided to use a tuned shock-excited transformer, as indicated in the figure. An automotive spark coil and spark module were selected for the high-voltage power supply, triggered at about 100 Hz by a signal generator. The coil output was rated at 30 kV with a rise time of $\sim 100 \mu\text{s}$, and it supplied adequate energy for this application. The high-voltage supply charges the capacitor C_1 through the primary L_1 of the transformer. When the breakdown potential is reached, conduction across the spark gap occurs. The primary $L_1 C_1$ circuit then resonates and is damped by dissipative losses. Oscillations are induced in the secondary $L_2 C_C$ circuit, where C_C represents the capacitance of the chamber. To maximize energy transfer and to reduce distortions, the primary and secondary circuits are independently tuned to the same resonance frequency. A number of tests were carried out to investigate the effects of the inductance, turn ratios, and different wire diameters and materials on the performance of the device.

Stray inductances and capacitances can cause significant problems. The large RF noise from the spark gap precludes direct observation of the voltage signal across the chamber with an oscilloscope. However, placing the scope probe close to the chamber and observing the induced signal gives a good indication of the shape, frequency, and decay time of the signal impressed on the chamber. If the tuning is accurate, the signal is a damped sine wave. The peak of the second oscillation is typically $\sim 15\%$ lower than the first. Further investigation has indicated that the electronic excitation comes primarily from the first cycle.

As the gas pressure in the chamber is increased from ~ 30 mtorr to near atmospheric, typical discharge regions are observed without the alpha source present. From no discharge at the lowest pressures, the onset of a glow is

seen as the pressure is increased. Further pressure increase results in well-defined sparks, until the pressure reaches a level at which the chamber no longer continuously conducts. When an alpha-particle track is present, tracks of brilliant streamers, consisting of discharges across the chamber, are observed at pressures where random sparks occurred before. At still higher pressures, where random spark discharges and streamers disappear, alpha-particle tracks are seen as a diffuse blue glow. The gas pressure for optimal track formation is critical and slight changes in E/P are very significant.

Because there is no triggering mechanism to start the RF field in response to the entry of an alpha particle into the chamber, tracks are seen at random times, on the order of seconds apart. Although readily visible to the eye, the tracks are difficult to photograph. In order to increase the film speed, the film was pre-exposed before exposing it to the light from the alpha tracks. Exposures were made by holding the camera shutter open and then closing it after visual observation of a track. Upon developing, most negative frames showed nothing, due to the low levels of light. A few showed discernible tracks. Prints of these, however, did not show a clear image of a track above the pre-fogged background (e.g., upper left frame in Fig. 3). With the assistance of the Electrical Engineering Department of the University of Tennessee and Perceptics, Inc., the track images were digitized and enhanced, enabling results similar to those shown in Fig. 3 to be obtained. The upper-right panel in Fig. 3 was obtained by enhancement with 256 shades of gray. The two bottom panels (identical) were generated from the latter, using only two shades, black and white.

An Optical, Digital Ionization Detector for Microdosimetry

Given the "proof-of-principle" observation and the imaging of alpha-particle tracks by optical detection, we turn next to the development of an instrument for making microdosimetric measurements. Its main features, which are shown schematically in Fig. 4, have been published previously⁽³⁾. An ionizing particle leaves a track of secondary electrons between the electrodes, as indicated. The particle also excites gas molecules, which promptly emit a small burst of optical radiation through the decay of excited states. This fluorescence radiation is detected by two wide-angle, fast, high-sensitivity photomultipliers, which feed signals into a fast discriminator coincidence detector. If the two photomultiplier pulses are detected within a given coincidence window time ($\lesssim 50$ ns), then the detector produces a trigger pulse for the RF field. The trigger pulse is fed into a master timing circuit which, in turn, triggers a high-voltage RF generator, producing the exciting field across the electrodes.

As already mentioned, the intensity of the light emitted depends on the magnitude and duration of the RF burst. The gas should have a high ionizing efficiency (low ionization threshold and low W value) and, more importantly, a high quantum yield for prompt (<10 ns) UV-to-visible radiation. Calculations show that the amplitude and duration of the RF burst can be chosen so that every electron in a track will emit a detectable pulse of light when observed by a camera from any direction.

From observation of the emitted radiation, we envision using two two-dimensional digital cameras, as shown in Fig. 4, which simultaneously view the light output across two perpendicular planes. The cameras could be either silicon-intensified vidicon cameras or microchannel plate-intensified, charge-coupled devices (or similar semiconductor cameras). Large pixel arrays are

required to accurately image the optical radiation from chamber, the resolution being proportional to the size of the pixel arrays in the cameras. The cameras are triggered by a pulse from the master timing circuit. They have adjustable exposure times (10 ns to 1 ms) to ensure that at least one detectable photon is recorded by both cameras for every electron in the track. The two cameras image the track in the two perpendicular planes and digitally store the information. The information is then transferred to a computer for analysis and track reconstruction.

After the imaging of a track is completed, a small DC clearing field is applied to clear the electrons and positive ions out of the chamber. The detection circuits are finally reset to record the next particle. The "cycle time" of the instrument will be on the order of ≈ 10 ms, so that about 100 events per second could, in principle, be measured. In practice, however, this pace of data acquisition would far outstrip the rate of transfer and analysis. Perhaps one event per second would be a reasonable rate for taking data.

Potential Uses of an Optical Digital Track Detector

The design of a particular chamber to be built would depend upon its intended use. We are now constructing a prototype neutron monitor. The principal track information needed is the energy deposited by an event and the corresponding track length. The energy is proportional to the total light output or the intensity and, under Bragg-Gray conditions, provides a measure of the absorbed dose in the wall of the chamber. The LET (in the gas) is the ratio of the energy deposited and the track length; it is needed to obtain the quality factor and the dose equivalent for the event. Moreover, one does not really need to know the LET when it is large. A quality factor of 20 can be

assigned when $LET > 175 \text{ keV}/\mu\text{m}$ in water. The unfolding of dosimetric information from recorded optical data appears to be relatively straightforward. In fact, successful algorithms for this purpose, utilizing an analogous digital neutron chamber design, have been worked out in detail⁽⁴⁾.

Different demands would be placed on a chamber to be used for microdosimetric measurements. A primary objective of such an instrument would be to measure actual electron positions in a track in a gas, analogous to the calculated positions in water in Fig. 1. The detector would thus give the spatial distribution of events and patterns of energy distribution by the charged particle and all of its secondaries. Calculations indicate that, with present know-how and with presently available (but expensive) digital cameras, it should be possible to image electrons in a track with a position uncertainty of $\sim 1 \text{ mm}$ in a gas at a pressure of about 5 torr. This resolution translates to $10 \times 10^{-7} \text{ g}/\text{cm}^2$, or $\sim 10 \text{ nm}$ in unit density material. (The diameter of the DNA double helix is $\sim 2 \text{ nm}$.) Thus the potential exists for measuring energy deposition in such small volumes, opening up the field of nanodosimetry.

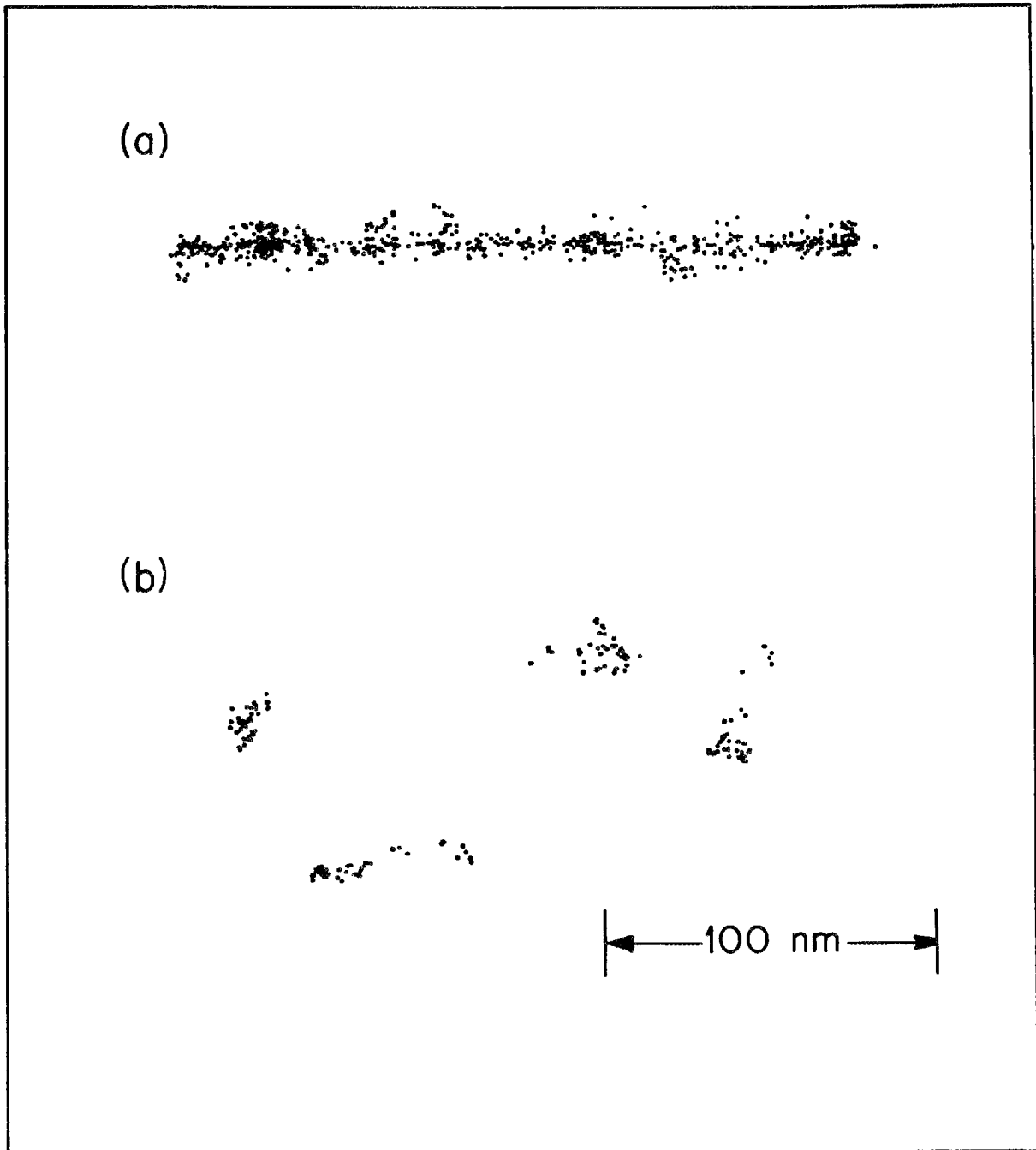
In addition to neutron dosimetry and microdosimetry, an optical detector would have other immediate applications. A number of important quantities for radiation physics could be determined on a track-by-track basis: W values, Fano factors, and energy-loss straggling distributions. Such a detector could also be used for three-dimensional characterization of laser and X-ray beams.

In another potential application, as mentioned in the Introduction, there is considerable discussion of using microdosimetric distributions rather than LET to characterize radiation quality for protection purposes. An improved

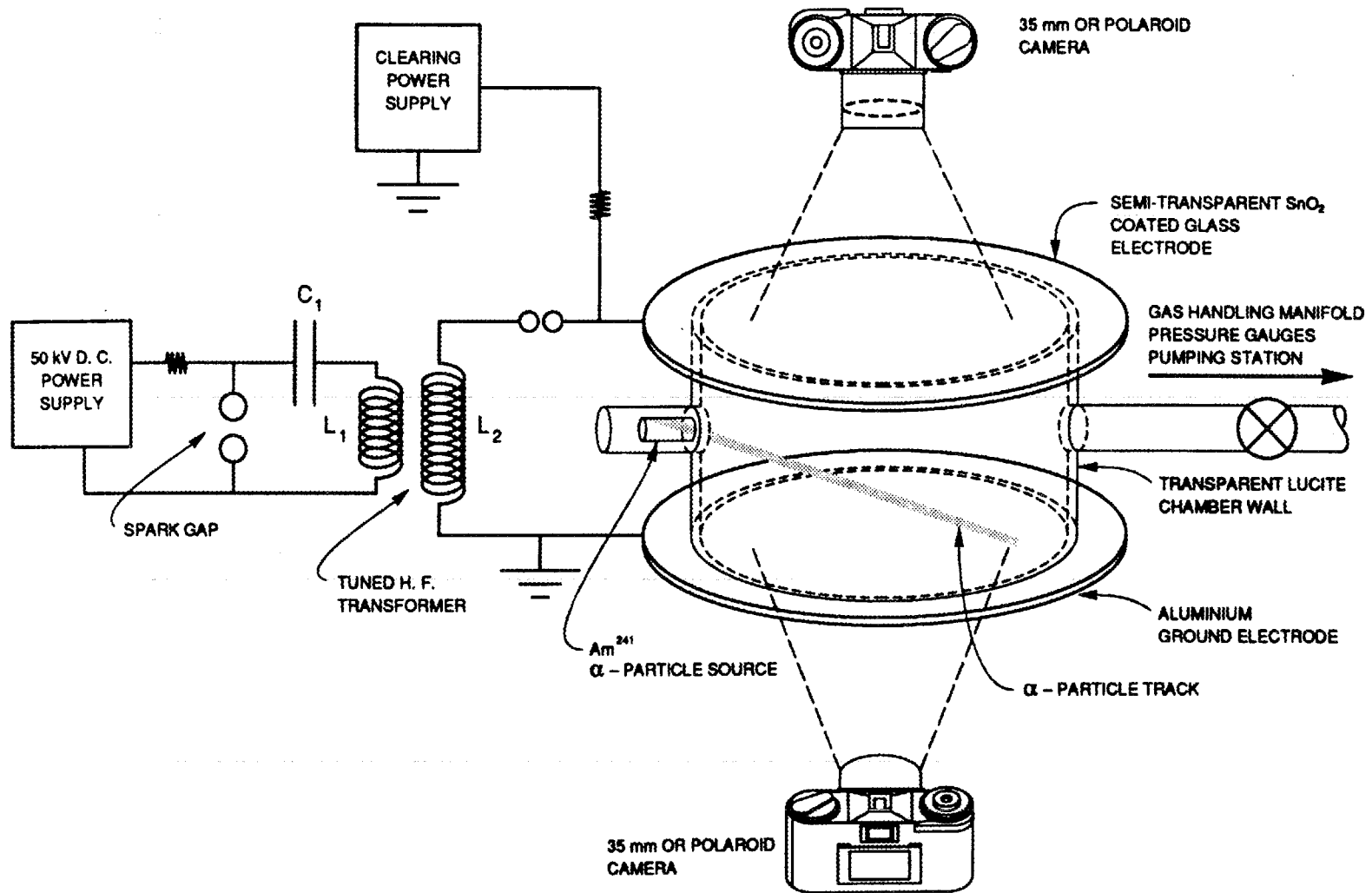
operational capability to measure such distributions could have an influence on the formulation of such standards as well as their technological implementation.

References

1. Microdosimetry, ICRU Report 36, International Commission on Radiation Units and Measurements, Bethesda, Maryland (1983).
2. Hamm, R. N., Turner, J. E., Ritchie, R. H., and Wright, H. A., Calculation of Heavy-Ion Tracks in Liquid Water, *Radiat. Res.* 104 (1985) S20 - S-26.
3. Hunter, S. R., Evaluation of a Digital Optical Ionizing Radiation Particle Track Detector, *Nucl. Instr. Meth.* A260 (1987) 469-477.
4. Bolch, Wesley, E., Turner, J. E., Hamm, R. N., Wright, H. A., and Hurst, G. S., A Method of Obtaining Neutron Dose and Dose Equivalent from Digital Measurements and Analysis of Recoil-Particle Tracks, *Health Phys.* 53 (1987) 241-253.



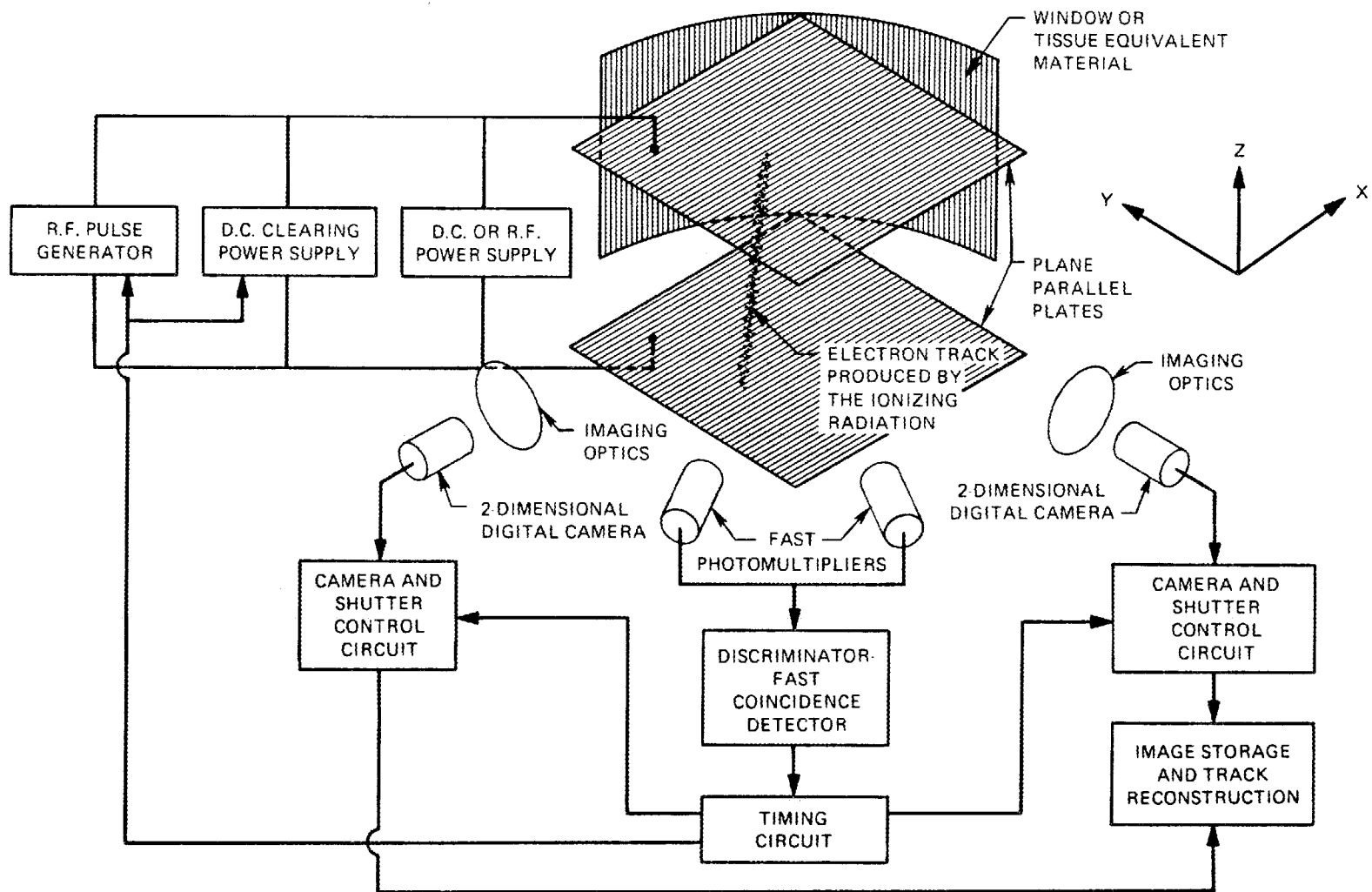
1. (a) Calculated track segment of a 5-MeV alpha particle in liquid water showing (dots) the locations of all subexcitation electrons (energies <7.4 eV) at 10^{-15} s after passage of the particle.
(b) 1-keV electron tracks in liquid water at 10^{-15} s.



2. Schematic diagram of the proof-of-principle device for observing alpha particles by optical means.



3. Upper left: Photograph of alpha-particle track. Upper right: Digitally enhanced photo of same by using scale with 256 shades of gray. Bottom panels (same): Further digital enhancement of upper-right panel with only black/white scale.



4. Schematic diagram showing principal components of an instrument that could be used for measurements in microdosimetry and other fields. From Ref. (3).

APPENDIX B

"DIGITAL CHARACTERIZATION OF RECOIL CHARGED-PARTICLE TRACKS
FOR NEUTRON MEASUREMENTS"

J. E. Turner, S. R. Hunter, R. N. Hamm, H. A. Wright
Oak Ridge National Laboratory
Post Office Box 2008
Oak Ridge, Tennessee 37831-6123

G. S. Hurst and W. A. Gibson
Pellissippi International
10521 Research Drive
Knoxville, Tennessee 37932

Accepted for publication in *Nuclear Instruments and Methods A*

DIGITAL CHARACTERIZATION OF RECOIL CHARGED-PARTICLE TRACKS
FOR NEUTRON MEASUREMENTS¹

J. E. Turner, S. R. Hunter, R. N. Hamm, H. A. Wright
Health and Safety Research Division
Oak Ridge National Laboratory
Oak Ridge, Tennessee 37831-6123 USA

G. S. Hurst, and W. A. Gibson
Pellissippi International
10521 Research Drive
Knoxville, Tennessee 37932 USA

Abstract

We are developing a new optical ionization detector for imaging the track of a charged neutron-recoil particle in a gas. Electrons produced in the path of the recoil particle are excited by an external, high-voltage, RF, electric field of short duration. Their oscillatory motion causes ionization and excitation of nearby gas molecules, which then emit light in subsequent de-excitation. Two digital cameras image the optical radiation across two perpendicular planes and analyze it for the numbers of electrons in various volume elements along the track. These numbers constitute the digital characterization of the track. This information can then be used to infer the energy deposited in the track and the track LET in the gas. We have now observed alpha-particle tracks in a chamber utilizing these principles. The application of such a device for neutron dosimetry and neutron spectrometry will be described.

¹Research sponsored by the Office of Health and Environmental Research and the Office of Nuclear Safety, U.S. Department of Energy, under contract DE-AC05-84OR21400 with Martin Marietta Energy Systems, Inc., and by the National Cancer Institute under Grant SSS-X(E) 1R43 CA45869-01 with Pellissippi International.

1. Introduction

This paper is about a new approach to making neutron measurements. Neutrons are important in a wide variety of activities, ranging from basic nuclear physics to industrial and medical applications. In many installations, neutrons present unwanted problems, such as the direct exposure of personnel and the activation of equipment and structural materials. Such problems exist, for example, at many accelerator facilities. The work presented here grew out of the need for improved monitoring and dosimetry for persons occupationally exposed to neutrons.

2. Statement of the Problem

Given a neutron field, knowing the fluence rate as a function of neutron energy and solid angle at every point in space and time would, in principle, provide sufficient information about the neutrons for all practical purposes. The data would provide directly, for example, scattering cross sections in an experiment with a parallel beam of monoenergetic neutrons. For dosimetry, the data could be used to calculate, and thus determine indirectly, the absorbed dose or energy deposited per unit mass in tissue exposed to the neutron field. In fact, knowledge about the secondary recoil charged particles produced by the neutrons in tissue is of more direct relevance for dosimetry, as presently practiced, than knowledge about the neutron field itself.

For radiation protection purposes, regulations specify that one evaluate the dose equivalent to a person exposed to radiation. This quantity is the product of the absorbed dose (energy absorbed per unit mass) and the appropriate quality factor for the radiation. The latter is defined in terms of the linear energy transfer (LET) of an incident or recoil charged particle in water [1]. Unfortunately, no general solution exists for the technical

problem of determining the energy deposited and LET of recoil events in tissue exposed to a neutron field. While there are definite successes, many aspects of neutron dosimetry remain an art.

3. Ionization Methods

Neutrons can be detected in a number of ways. Slow neutrons ($\lesssim 0.5$ eV) can activate foils and, when absorbed by a nucleus, can produce energy-releasing reactions, such as $^{10}\text{B}(n,\alpha)^7\text{Li}$, which can be readily detected in a scintillator or proportional counter. Intermediate (up to ~ 0.1 MeV) and fast ($\gtrsim 0.1$ MeV) neutrons produce, through elastic scattering, charged recoil particles that can be monitored with proportional counters. They also activate foils, typically selected with certain thresholds to provide neutron spectral information. Intermediate and fast neutrons can also be moderated first and then detected as slow or thermal neutrons by capture reactions.

Neutrons show a variety of interactions, and their cross sections are notoriously energy dependent. Of the two quantities required for dosimetry - the absorbed energy and the LET (or quality factor) - the former is more accessible to direct measurement. For example, a proportional-counter probe can be made with tissue-equivalent plastic walls enclosing a tissue-equivalent gas. If the wall thickness allows for secondary charged-particle equilibrium with the gas, and if other conditions of the Bragg-Gray principle are met, then the neutron dose in the walls can be obtained simply by measuring the pulse-height spectrum from the gas ionization.

Ionization in a gas provides a very sensitive and versatile process for radiation detection and dose measurement, and it is the basis for the digital approach, which we describe next.

4. The Digital Approach

Figure 1(a) shows the calculated track of a 1-MeV proton traversing a cylindrical volume, representing the probe of a proportional counter. The cylinder has a diameter of 5 cm and a length of 8 cm, and the track is in a plane containing the cylinder axis. The proton could have been produced under Bragg-Gray conditions in a wall surrounding the cylinder. The dots show the positions of the subexcitation electrons produced directly by the proton or one of its secondaries immediately after passage through the counter, before the electrons have drifted appreciably. Figure 1(b) shows the track of a 22-keV carbon ion entering the gas from the wall. This track is also in a plane containing the axis of the cylinder. As described in the caption, the two events, (a) and (b), produce about the same number of electrons. However, the carbon ion expends more energy than the proton, because of its higher W value (average energy per ion pair) as it stops. Operated as a proportional counter, this dosimeter would register comparable pulse heights from the two events, implying comparable doses. Also, the measurements would not indicate what quality factors should be assigned to the events. The calculations show that the average LET for this proton track segment is $200 \text{ MeV cm}^2/\text{g}$, for which a quality factor $Q \approx 4$ is appropriate. The LET for the C recoil is $1200 \text{ MeV cm}^2/\text{g}$, corresponding to $Q \approx 18$. The missing piece of information about neutron recoil events in a proportional counter is the track length in the gas.

Several approaches beyond this point have been proposed. H. H. Rossi pioneered the use of spherical proportional counters to measure LET spectra [2]. The isotropic chord-length distribution in the sphere is a simple analytic function, and one can statistically relate an event size with a track length. However, if a significant fraction of the recoil particles stop or

start within the chamber, the track-length distribution will not be well approximated by the chord-length distribution. We devoted considerable effort to an iterative unfolding of LET spectra for a standard, cylindrical proportional counter, for which the chord-length distribution can be compiled numerically [2]. These methods have met with some success for energetic neutrons, but they still fall short of giving sufficiently accurate LET distributions in many cases. Position-sensitive proportional counters are also available, but they are sophisticated and costly for dosimetric purposes. On the other end of the spectrum, completely analogue "rem meters" exist to obtain neutron dose equivalent directly. However, their response is only approximate and is tied explicitly to currently defined quality factors.

At this point, we can ask a very fundamental question: What is the most information that one can have about a particle track in a gas? The particle leaves a number of subexcitation electrons, excited molecules, and positive ions in its wake. Short of knowing everything about a track, one can still learn a great deal by measuring the numbers of electrons in various volume elements spanning a chamber volume. In this fashion, a particle track would be characterized digitally as a set of integers, each associated with a given volume element of the chamber and providing the number of electrons in that element.

For dosimetry, the total number of electrons in tracks such as those in Fig. 1 would provide the absorbed energy, since the W values are known. Moreover, knowledge of the specific volume elements which contain electrons would enable the track length to be determined. The LET is then the ratio of the energy absorbed and the track length.

5. An Optical Electron Detection Technique

The most promising principle for obtaining digital data from tracks appears to be the detection of optical radiation from gas molecules excited in the immediate vicinity of the electrons in a track [3]. The operation of this detector can be understood from Fig. 2, which gives a schematic representation of the initial device we have built and used to see tracks from a ^{241}Am source, which emits 5.5-MeV alpha particles. Immediately after passage of an alpha particle, electrons in the track are excited by application of an external, high-frequency, high-voltage pulse applied across two parallel disc electrodes with the track between. The RF field causes the electrons to oscillate rapidly, gaining sufficient energy to ionize and excite the gas molecules in their immediate vicinity. The duration of the pulse is limited so that an avalanche onset does not occur. The excited gas molecules produce copious numbers of photons by fast fluorescent decay. The intensity of the light from different regions is proportional to the number of electrons there. The alpha-particle tracks can be readily seen by the naked, dark-adapted eye. Figure 3 shows a photograph of an alpha-particle track in the device.

The cylindrical chamber in Fig. 2 is about 3 cm in height and 10 cm in diameter. It was operated at pressures between 300 and 600 torr with various gases and mixtures, such as N_2 , Ar, Ar + N_2 , Ar + Xe, and Ar + TMAE [tetrakis (dimethylamine) ethylene]. A potential difference of ~ 10 kV was used at an operating frequency of 5-15 MHz and a pulse repetition rate of ~ 100 Hz. The best spatial resolution was visually judged to be about 1-2 mm in the direction perpendicular to that of the applied field and about 2-4 mm parallel to the field. The light intensity is highly dependent on gas composition and pressure as well as the voltage level of the RF pulse. Calculations confirm

our observation that operation of the detector with small percentages (1-5%) of Xe or N₂ in Ar gives the best performance in terms of spatial resolution and light output from the track.

In going from this initial "proof-of-principle" device to a useful dosimeter or other device, a considerable amount of additional work remains to be done. For example, a triggering device is needed to turn on the field in response to the entrance of a particle, e.g. by using the natural fluorescence of the gas. Fast switching circuitry and triggerable RF voltage pulses of higher frequency and longer length must be developed. We also need to explore methods of limiting electron diffusion (e.g., by negative-ion formation), particularly at low pressures. The output itself requires computer hardware and software to record the track images and analyze them to extract the required information. We are investigating the use of two digital cameras to simultaneously scan and image the emitted light across two perpendicular planes outside the chamber. We developed an algorithm to unfold the digital data from an earlier version of the chamber and showed that it worked very successfully for determining dose and dose equivalent for neutron dosimetry [4]. In the longer term, we need to understand the basic physical processes and energy pathways that determine how the detector operates in order to optimize and fully utilize it.

An important characteristic of the device represented in Fig. 2 is that major variables, such as gas composition and pressure, RF pulse amplitude, frequency and duration, can be controlled externally and hence changing them does not require rebuilding a chamber.

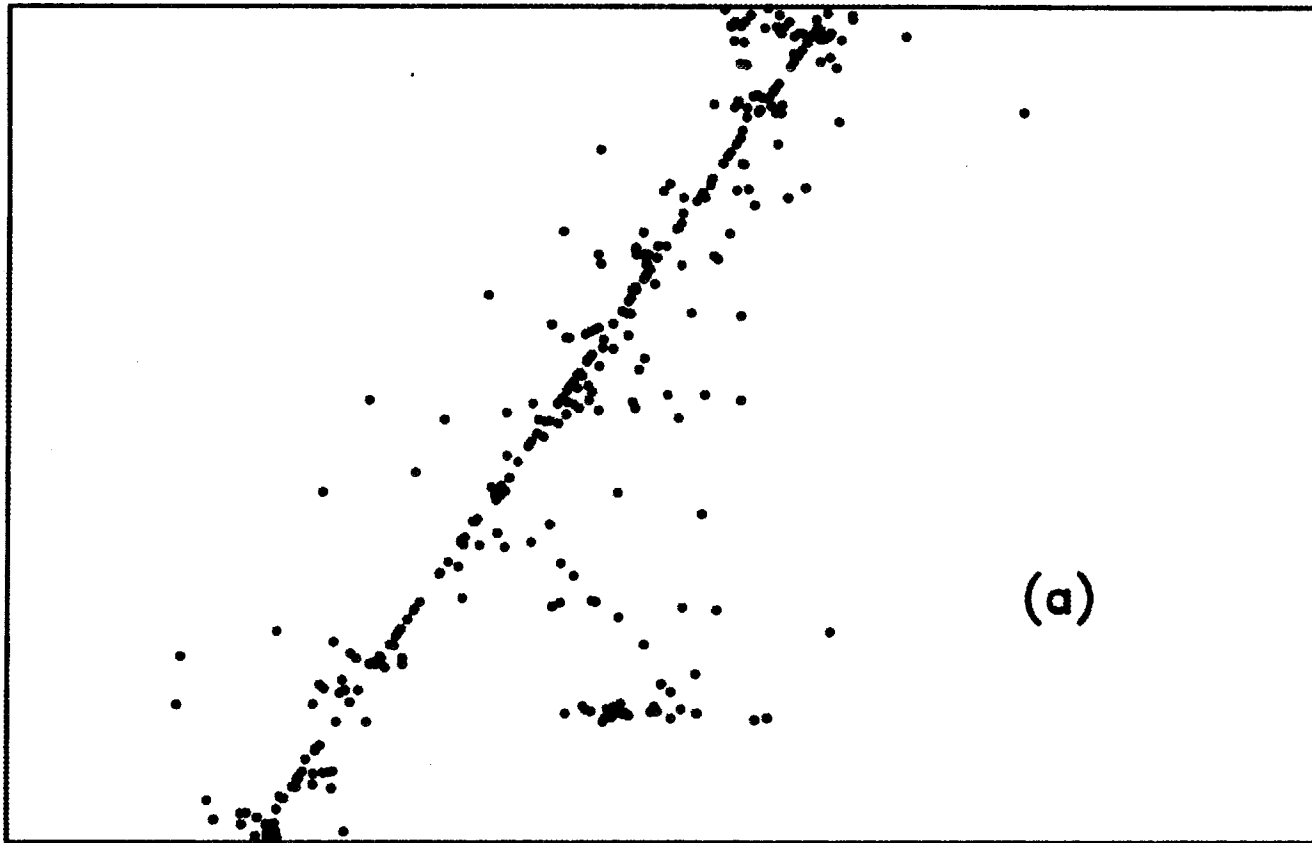
Summary

We have described a digital concept for particle-track characterization and a prototype device that has demonstrated the needed track visualization. This basic approach has the potential for a variety of uses in addition to neutron dosimetry. One could make measurements of range and energy-loss straggling. Track-structure calculations could be checked experimentally. W values and Fano factors could be obtained on a track-by-track basis. Its potential as a neutron spectrometer has yet to be explored. Such a device could also be considered for 3-dimensional imaging of laser and X-ray beams.

References

- [1] Recommendations of the ICRP, ICRP Publication 26 (International Commission on Radiological Protection, Pergamon Press, Elmsford, New York, 1977) p. 4.
- [2] Microdosimetry, ICRU Report 36 (International Commission on Radiation Units and Measurements, Bethesda, Maryland, 1983) pp. 64-68.
- [3] S. R. Hunter, Nucl. Instr. Meth. A260(1987) 469.
- [4] W. E. Bolch, J. E. Turner, R. N. Hamm, H. A. Wright, and G. S. Hurst, Health Phys. 53(1987) 241.

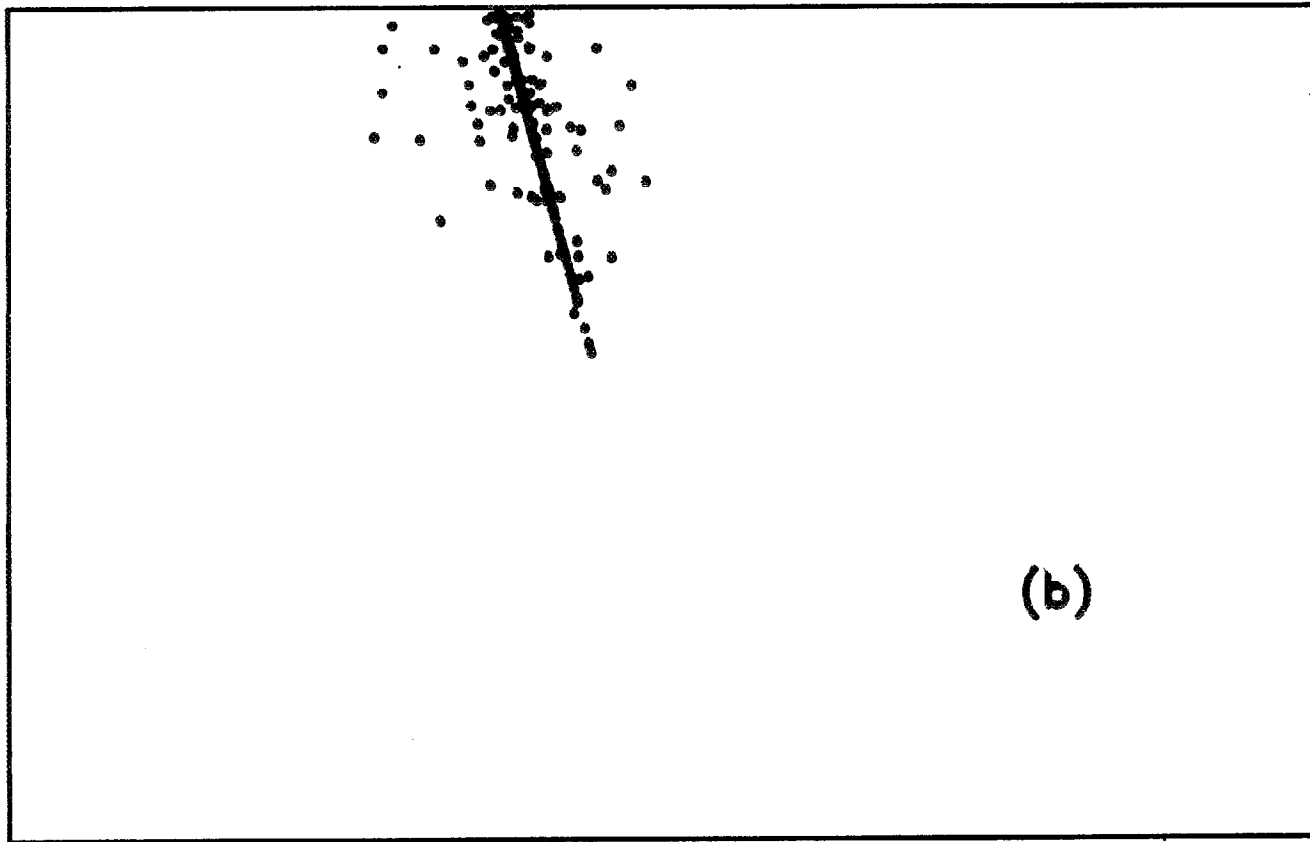
5 cm



8 cm

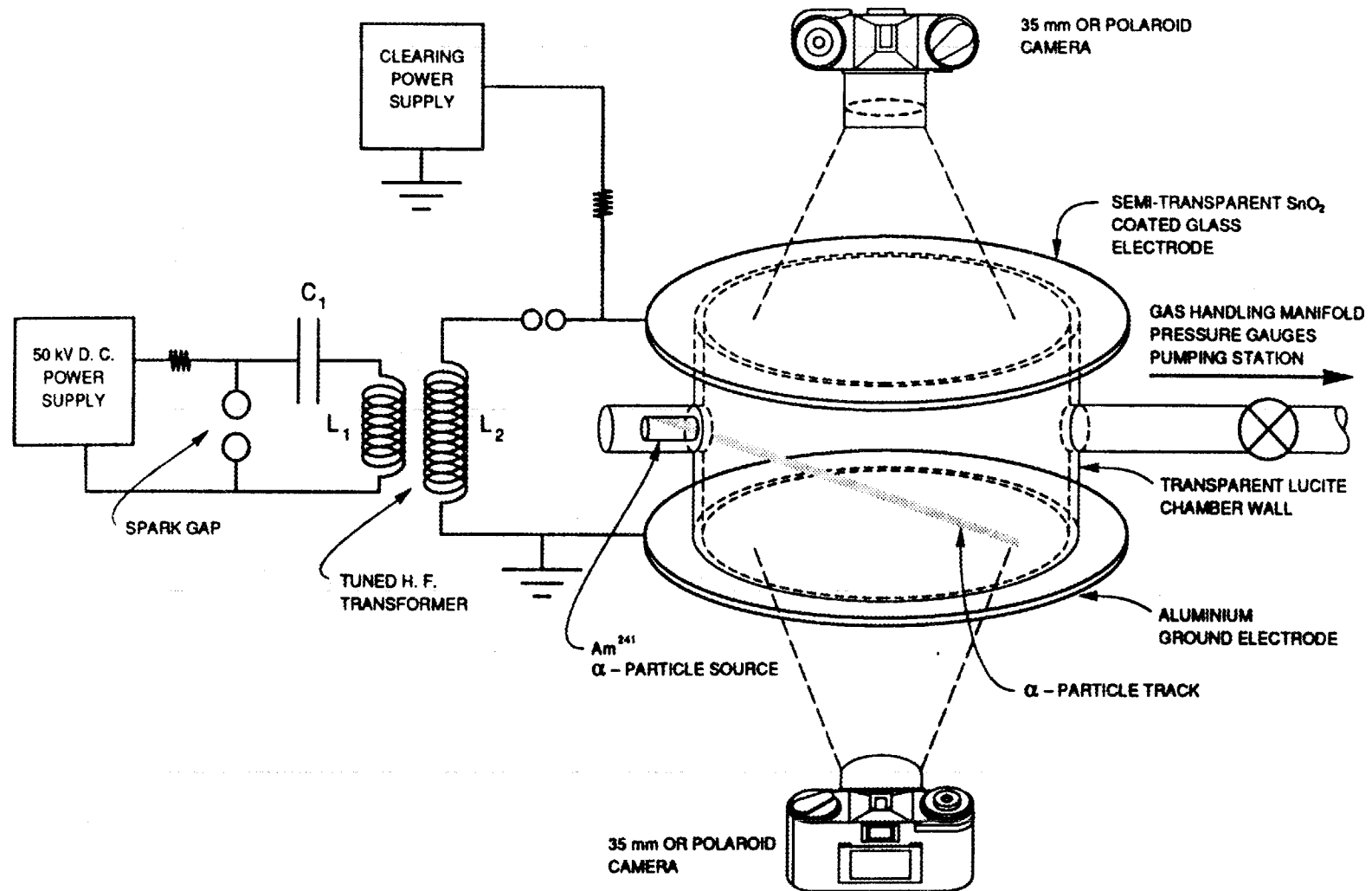
Fig. 1. (a) Calculated track of a 1-MeV proton crossing a Bragg-Gray chamber filled with CH_4 at 5 torr. This track produced 352 electrons, each represented by a dot. The proton lost 10.4 keV in the gas.

5 cm



8 cm

- (b) A 22-keV carbon recoil ion from the wall of the same chamber.
It produces 341 electrons and stops in the gas.



63

Fig. 2. Schematic diagram of initial device in which alpha-particle tracks can be seen.

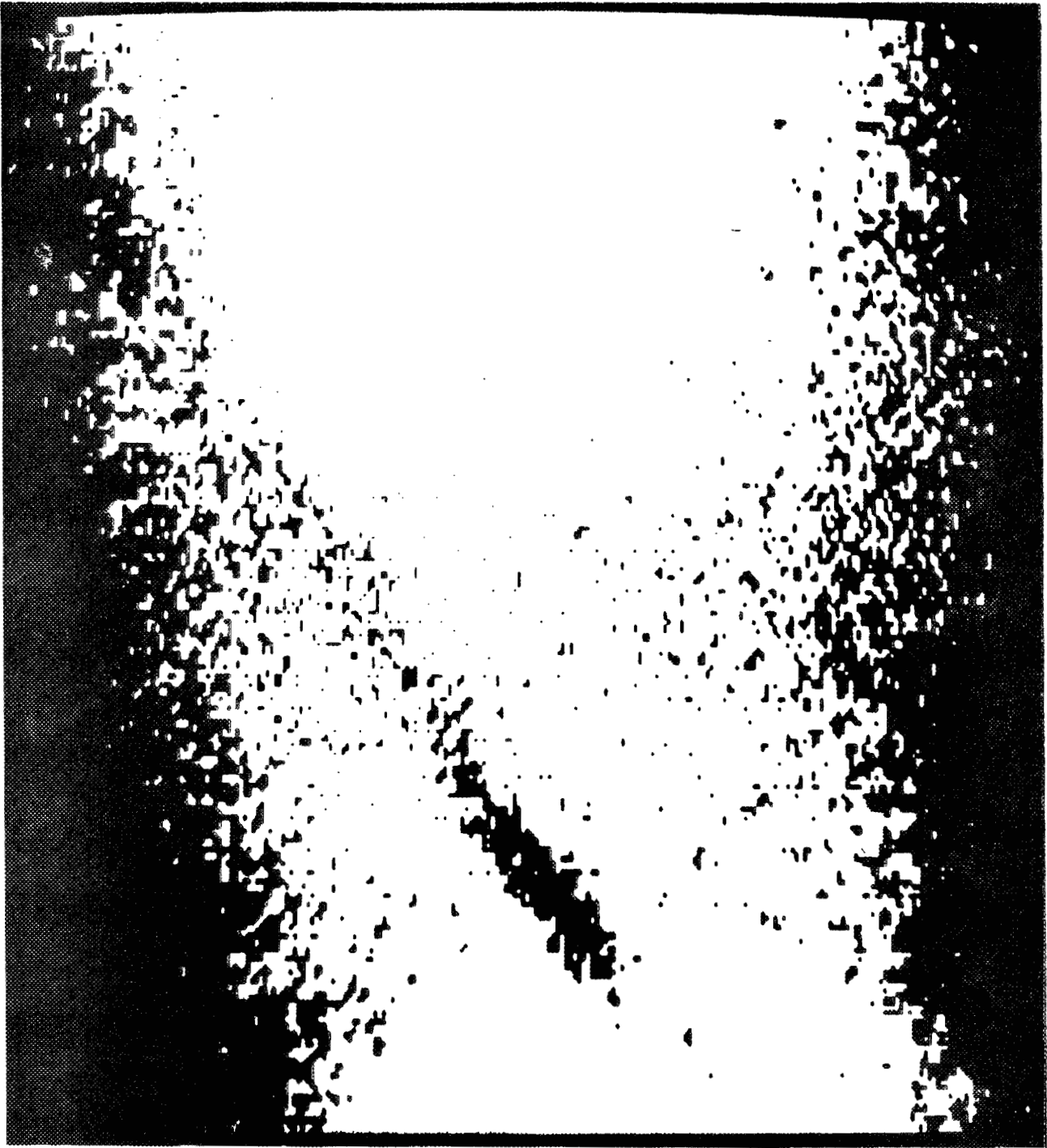


Fig. 3. Digitally enhanced photograph of alpha-particle track in chamber, showing the change in track density as the particle slows down and stops near the center of the chamber.

INTERNAL DISTRIBUTION

1. J. G. Carter
2. L. G. Christophorou
- 3-4. R. N. Hamm
- 5-7. S. R. Hunter
8. S. V. Kaye
9. L. A. Pinnaduwege
10. I. Sauers
- 11-12. J. E. Turner
- 13-14. H. A. Wright
- 15-16. Central Research Library
17. Document Reference Section
- 18-19. Laboratory Records Department
20. Laboratory Records Department - RC
21. ORNL Patent Office

EXTERNAL DISTRIBUTION

22. L. G. Faust, Health Physics Department, Battelle Pacific Northwest Laboratories, P. O. Box 999, Richland, Washington 99352.
- 23-24. W. A. Gibson, Pellissippi International Inc., 10521 Research Drive, Suite 300, Knoxville, Tennessee 37932
25. G. S. Hurst, Institute of RIS, 10521 Research Drive, Suite 300, Knoxville, Tennessee 37932
26. S. M. Lawless, Battelle Pacific Northwest Laboratories, P. O. Box 999, Richland, Washington 99352
27. M. O. Pace, Department of Electrical Engineering, University of Tennessee, Knoxville, Tennessee 37996
28. C. M. Stroud, Health Physics Department, Battelle Pacific Northwest Laboratories, P. O. Box 999, Richland, Washington 99352
29. E. J. Vallario, Office of Nuclear Safety, EH-132, U.S. Department of Energy, Washington, D.C. 20545
30. M. Varma, Office of Health and Environmental Research, U.S. Department of Energy, Washington, D.C. 20545
31. R. W. Wood, Office of Health and Environmental Research, U.S. Department of Energy, Washington, D.C. 20545
- 32-33. Office of Assistant Manager for Energy Research and Development, DOE/ORO
- 34-43. Office of Scientific and Technical Information, P.O. Box 62, Oak Ridge, TN 37831